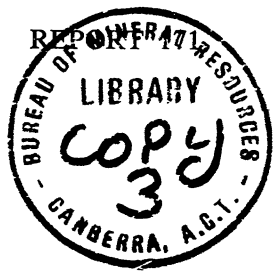

Environmental Significance of Folds in the Rangal Coal Measures at Blackwater, Queensland

W. A. Burgis

BMR PUBLICATIONS COMPACTUS
(LENDING SECTION)

DEPARTMENT OF MINERALS AND ENERGY
BUREAU OF MINERAL RESOURCES, GEOLOGY AND GEOPHYSICS

REPORT 171

Environmental Significance of Folds in the Rangal Coal Measures at Blackwater, Queensland

W. A. BURGIS

AUSTRALIAN GOVERNMENT PUBLISHING SERVICE
CANBERRA, 1975

DEPARTMENT OF MINERALS AND ENERGY

MINISTER: THE HON. R. F. X. CONNOR, M.P.

SECRETARY: SIR LENOX HEWITT, O.B.E.

BUREAU OF MINERAL RESOURCES, GEOLOGY AND GEOPHYSICS

ACTING DIRECTOR: L. C. NOAKES

ASSISTANT DIRECTOR, GEOLOGICAL BRANCH: J. N. CASEY

Published for the Bureau of Mineral Resources, Geology and Geophysics by the Australian Government Publishing Service

ISBN 0 642 00812 4

MANUSCRIPT RECEIVED: MAY, 1973

REVISED MANUSCRIPT RECEIVED: OCTOBER, 1973

ISSUED: MARCH, 1975

Printed by Graphic Services Pty Ltd, 86a Pirie Street, Adelaide 5000

CONTENTS

FIGURES

SUMMARY

The origin of domal structures and the vertical profile exposed in the Utah Development Company open-cut coal mine at Blackwater were studied to determine the palaeoenvironmental setting of the Upper Permian Rangal Coal Measures. The domes occur in beds above the productive coal seam, but do not affect it.

The vertical succession of beds in the coal measures is characteristic of that produced by a meandering river. The coal seams and interbedded fine clastic rocks formed on a flood plain. Lenses of clastic rocks in carbonaceous beds were originally deposited in small subsiding lake basins in a peat swamp. The basins probably developed initially in response to differential compaction of point-bar sand and muddy overbank sediment below the peat, and they continued to subside because of differential compaction of the peat seam itself. The basins filled with sediment when the rate of compaction below them decreased relative to the rate of compaction in adjacent areas. Peat was deposited over areas formerly occupied by lakes. The more slowly subsiding, relatively incompressible lenses of clastic sediment were domed as differential compaction continued, and the domes became mounds on the peat-covered surface. Lacustrine sediment was deposited in depressions around the hills, and developed into new mounds. Three generations of lakes developed on the flood plain before a river channel migrated back to the area to deposit point-bar sand over the lacustrine sediment.

Lower quality of coal and instability of mine walls are related in places to strata domed by differential compaction. Methods suggested by this study for predicting the location and geometry of compactional folds may be useful in planning pit design and mine development in coalfields where these structures are developed.

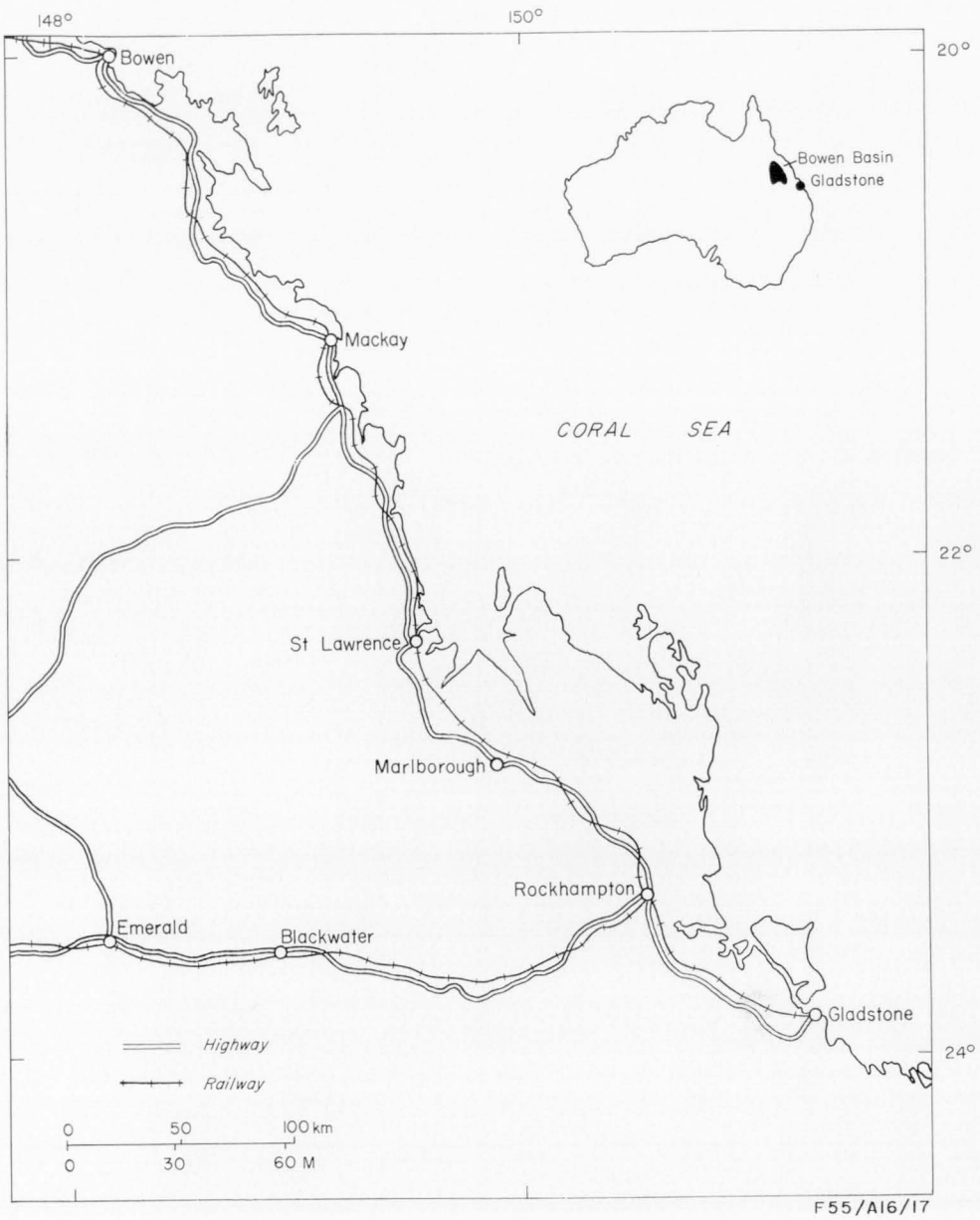

Fig. 1. Location of Blackwater.

INTRODUCTION

Geologists have had the opportunity of seeing large exposures of the Rangal and Baralaba Coal Measures only in the last decade when large-scale open-cut mining developed in the Bowen Basin. Cross-sections of the coal measures in mines at Moura and Blackwater, Queensland, show that the seams are interbedded with sandstone and shale which lie in anticlines and synclines. In incomplete sections the clastic rocks commonly resemble the foreset units of a small lacustrine delta. More complete sections, however, show the anticlinal nature of such beds; discordant folds at higher levels are separated from the lower structures by thin carbonaceous beds split from the main coal seams. This study aimed at determining the origin of the folds at Blackwater and whether they reflect a specific depositional environment. In this Report the terms fold, anticline, and syncline refer only to the geometry of structures and are not used in a genetic sense.

Blackwater is in central eastern Queensland, about 190 km west of Rockhampton (Fig. 1). The Upper Permian Rangal Coal Measures dip gently to the east and crop out in a north-trending belt west of Blackwater (Fig. 2). Miss W. A. Burgis and Mrs P. E. Simpson of the Bureau of Mineral Resources and Mr W. H. Koppe of the Geological Survey of Queensland investigated the Utah Development Company open-cut mine about 20 km south-southwest of Blackwater during June 1971.

A partial section of the Rangal Coal Measures is exposed in the mine. Detailed maps of 6 km of the highwall in the Deep Creek/Taurus and Stewarton pits (Fig. 3) were drawn on overlapping photographs in the field. Structural and lithological data were recorded on sketch maps of the walls of vehicle ramps and a drainage ditch. Direct access to the highwall was difficult, but measurement and description of complete highwall sections were possible in the two key-cuts (Fig. 3). Vertical sequences of types of stratification were analysed for the two sections. Palaeocurrent directions were measured wherever possible. Structure contour and isopach maps of carbonaceous horizons in the mine were plotted by computer from logs of 430 selected company drill holes, the distribution of which is shown in Figure 4.

Maps of the mine highwalls in June 1971 are presented in Figures 5 and 6. The highwalls have been divided into sections to facilitate reference in discussion. Specific localities within a section are designated by numbers in Figures 5 and 6. The Deep Creek/Taurus highwall is divided into the following sections: A, folded clastic rocks discordantly overlying the Argo seam; B, the Deep Creek/Taurus seam split; and C, clastic rocks between two carbonaceous shales. Section C continues in the Stewarton highwall, which is divided further into D, the Stewarton split between coal and carbonaceous shale; E, a broad anticline in clastic rocks interbedded with two carbonaceous shale units; and F, a large anticline discordantly overlying the Argo seam.

The Utah Development Company system of reference lines runs roughly perpendicular to the position of the highwall (Fig. 3) and has been related on all maps to boundaries of the highwall sections. A particular line is designated by its distance, recorded in units of 1000 feet (304.8 m), from the primary reference or C4 line. North of the C4 line the units are positive; south of it, they are negative.

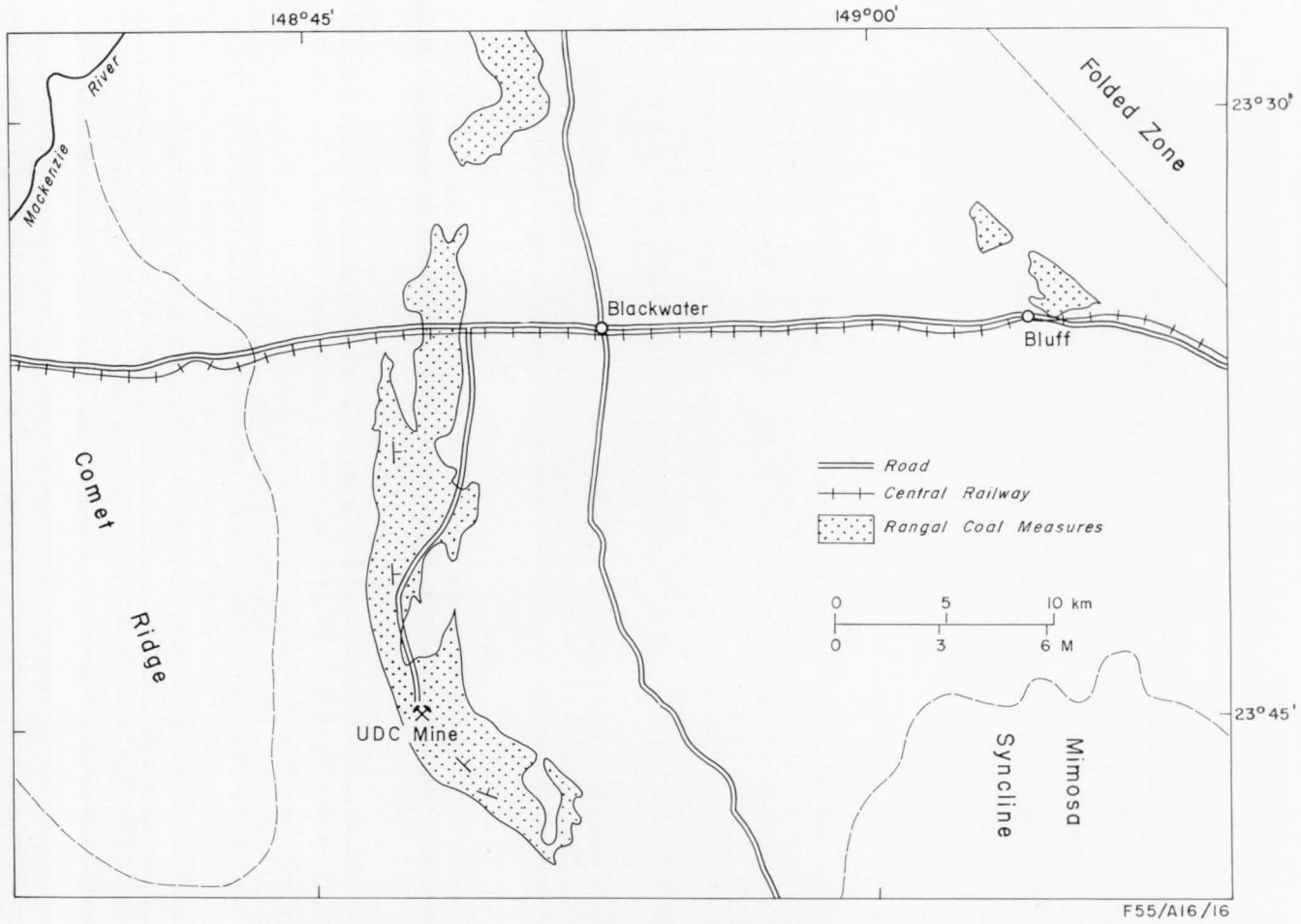

Fig. 2. Outcrop of the Rangal Coal Measures, Blackwater, Qld.

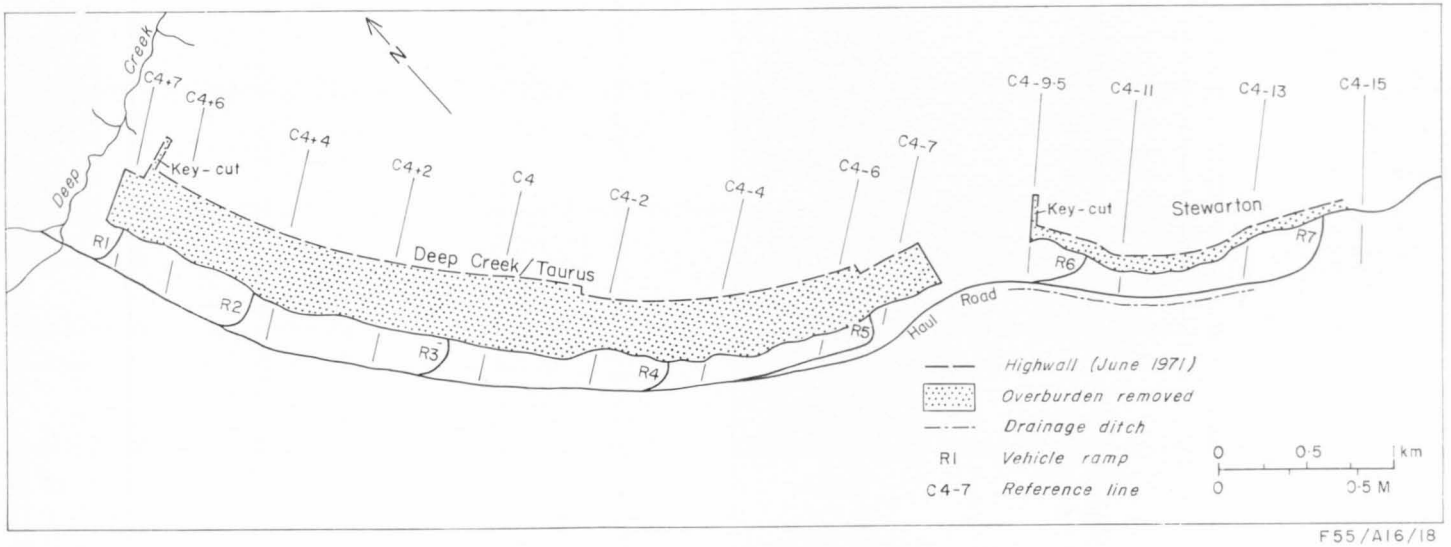

Fig. 3. U.D.C. mine plan, Blackwater, Qld.

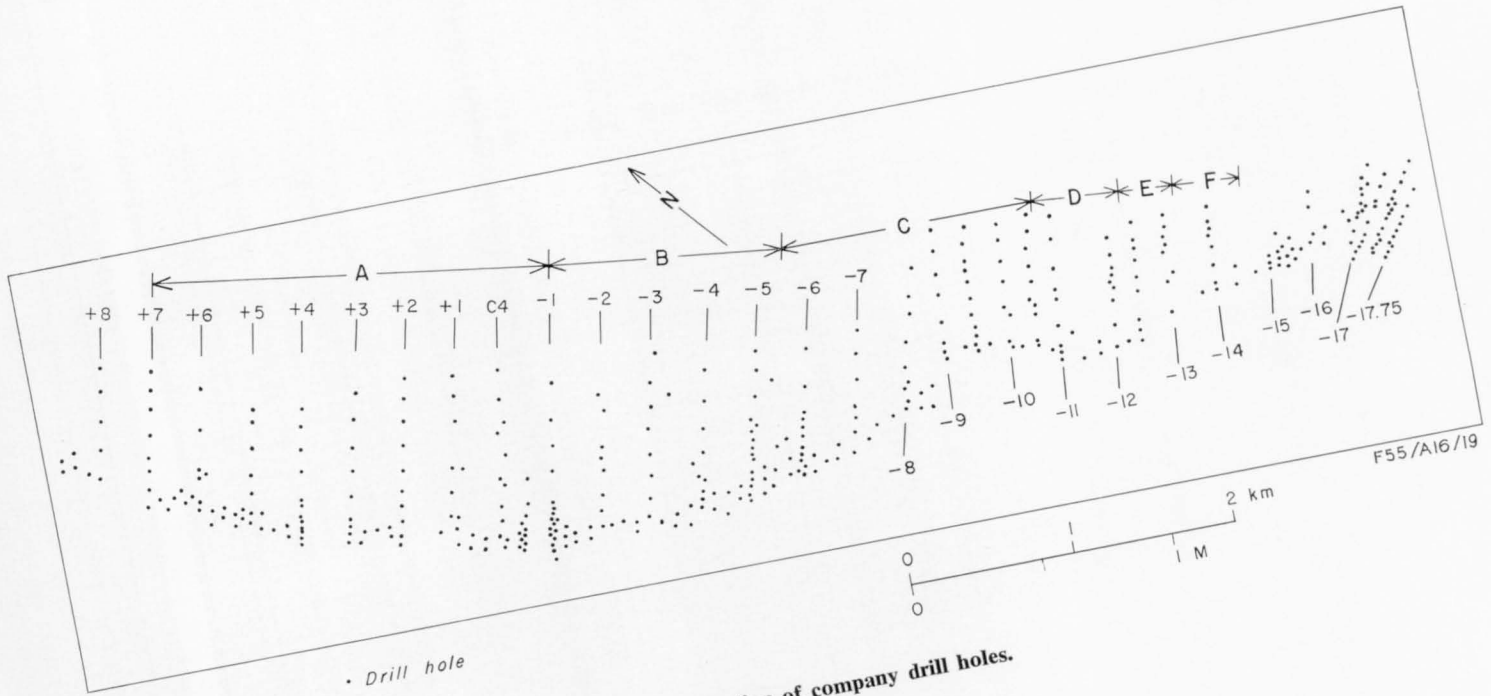

Fig. 4. Location of company drill holes.

ACKNOWLEDGMENTS

I am indebted to the management and staff of Utah Development Company at Blackwater for permission to work in the mine, access to company records, and hospitality. I am also grateful to Mr E. N. Milligan of Utah Development Company for suggesting economic applications of this study and to Dr S. Henley for developing the computer program used to produce structure contour and isopach maps.

GENERAL GEOLOGICAL SETTING

PREVIOUS INVESTIGATIONS

The geology of the Blackwater areas has been discussed in publications dealing with the Bowen Basin as a whole (Davis, 1971; Dickins & Malone, 1973) and with the Duaringa 1:250 000 Sheet area (Malone, Olgers, & Kirkegaard, 1969; Kirkegaard, 1970). Paten (1971) and Staines (1972) discuss the geology of the Blackwater coalfield, and unpublished Utah Development Company reports (King, Goscombe & Hansen, 1963; Hansen, 1965; Marshall & Tompkins, 1966) include detailed information about the stratigraphy of the mine area.

Folds similar to those at Blackwater have been attributed to compaction, sedimentation, and erosion in several depositional environments. Britten (1972) explains the development of mutually discordant folds in the Singleton Coal Measures of New South Wales by the differential compaction of peat and interbedded pods and wedges of clastic fluvial sediment. The highly variable conditions of sedimentation in a fluvial environment produce interbedded and interfingering bodies of sediment with very different compactional properties. Britten therefore feels that compactional folding and faulting are characteristic of coal-bearing fluvial sequences.

The origins of some folds similar to those at Blackwater have been related to specific facies of the fluvial environment. Large-scale sandstone cross-strata dip onto a coal seam in the Baralaba Coal Measures at Moura, Queensland. This discordance of sandstone and coal has been interpreted as representing the construction of a delta into a lake basin which subsided because of differential compaction of the underlying peat (Jensen, 1968). Raistrick & Marshall (1939) describe seam splits which have cross-sections identical with splits at Blackwater. The original depressions were river channels eroded into peat. When the channels were abandoned, they became oxbow lakes and filled with sediment. Peat grew over the channel-fill sediments, which evolved into high anticlinal bodies by compactional mechanisms similar to those proposed by Britten (1972) and in this Report for the development of splits at Blackwater. The channel-fill bodies are long and sinuous in plan view.

However, neither the lacustrine delta nor channel-fill model can completely explain the development of splits at Blackwater. The structural geometry and lithology of rocks above the coal at Moura are not exactly analogous to those at Blackwater. Furthermore, there is no sign of widespread erosion of the coal below

---

Footnote. In this Report the term 'sediment' (or 'sediments') means unlithified material.

the splits at Blackwater, and these features do not resemble river channels in plan view. Thus, the splits at Blackwater must have formed in a different specific depositional environment.

Williams (1971) concludes from a study of the Deep Creek/Taurus split (Fig. 5, B1 to B7) that the sedimentary rocks in this lens were deposited in a small basin which was produced by rapid subsidence of the peat in a local area.

Stratigraphy

The Rangal Coal Measures are the uppermost formation in the Upper Permian Blackwater Group in the central Bowen Basin. The Blackwater Group overlies the Blenheim Subgroup, which records a marine transgression into the Bowen Basin in Upper Permian time. The Blackwater Group consists of the Fair Hill Formation, Burngrove Formation, and Rangal Coal Measures in the Blackwater area. It is generally regarded as non-marine.

The Fair Hill Formation conformably overlies the German Creek Coal Measures and is composed of 85 to 135 m of sandstone, siltstone, mudstone, and minor beds of coal and carbonaceous shale. Marine fossils have not been found in the Fair Hill Formation. Jensen (1971, p. 13) concludes that '. . . the combination of sandstone with high-angle cross-stratification, pebble bands and abundant fossil logs, and interbedded sequences of laminated mudstone, suggests deposition in a fluvial environment.' Palaeocurrents which deposited the Fair Hill Formation flowed to the south-southwest.

The overlying Burngrove Formation consists of 90 m of cherty mudstone and hard siliceous siltstone with subordinate amounts of sandstone, tuff, carbonaceous shale, and coal. Plant remains are abundant, with fossil logs and tree-ferns restricted to the top of the unit. Fish and reptile trails are preserved in some localities. In contrast to the coarser-grained trough cross-stratified Fair Hill Formation, the Burngrove Formation consists of laminated regular beds; only small-scale cross-strata are present. Small-scale slump structures are common, and in places laminae are graded. The Burngrove Formation was deposited under quiet lacustrine conditions and grades conformably into the overlying coal measures.

The Rangal Coal Measures consist of mudstone, siltstone, labile sandstone, carbonaceous shale, and coal, and are 107 to 137 m thick near the Utah Development Company mine (Staines, 1972). The type section is along Deep Creek (Fig. 3) (Malone, Olgers & Kirkegaard, 1969). Sandstone is dominant in the lower part of the coal measures in the Blackwater area. The upper part of the formation changes facies northward from a shale-sandstone sequence near the Central Railway to dominantly sandstone near the Mackenzie River (Staines, 1972). The sandstone is moderately sorted, fine to coarse-grained, carbonaceous, and commonly cross-stratified. Rock fragments are dominantly of volcanic origin, but some sedimentary grains are present. Thin bedding and lamination are generally characteristic of mudstone in the coal measures.

The Rangal Coal Measures and their lateral equivalents, the upper part of the Baralaba Coal Measures, the Elphinstone Coal Measures, and 'Upper Bandanna' Formation, usually contain one thick coal seam or a number of moderately thick seams. Although they are commonly split, the seams can be traced over wide areas and change facies from coking to non-coking coal. The seam which the Utah Development Company is mining at Blackwater was formerly called the Main

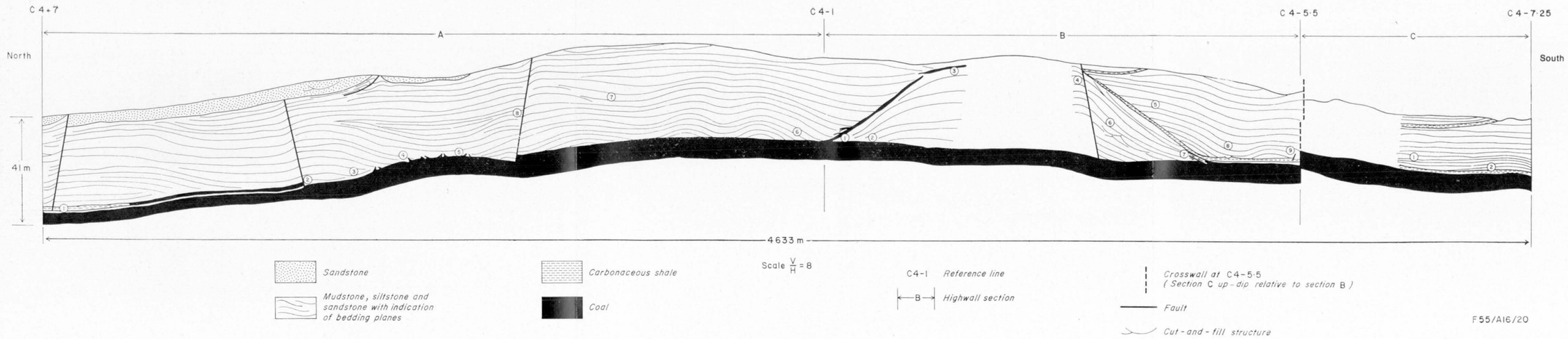

Fig. 5. Deep Creek/Taurus highwall, June 1971.

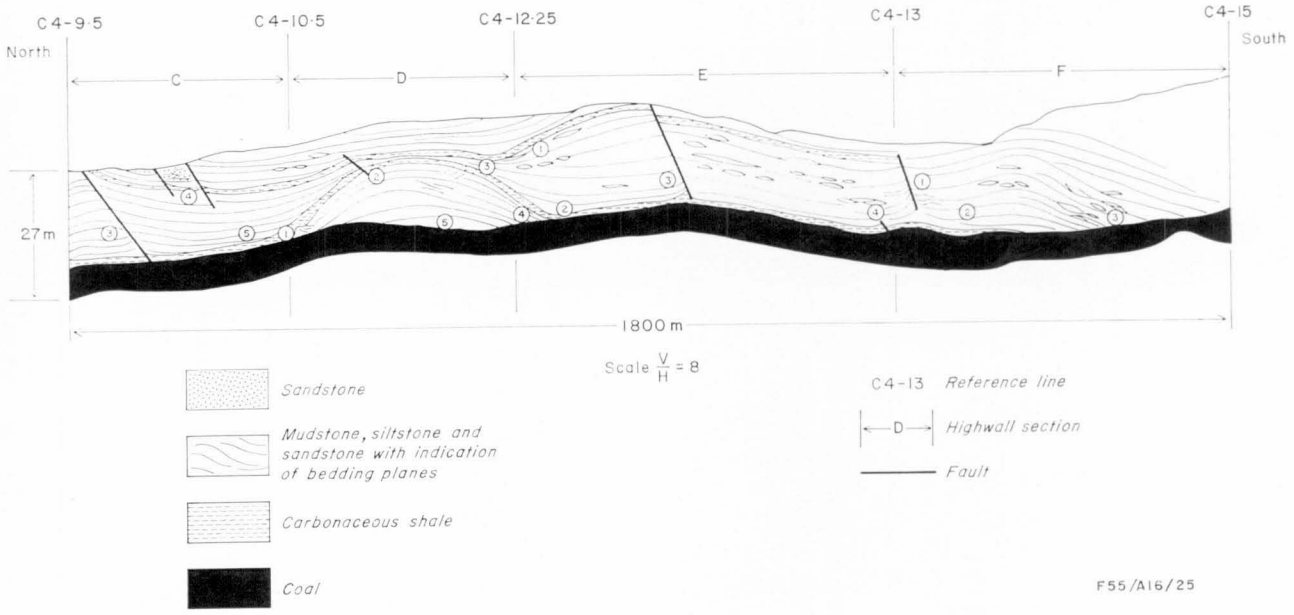

Fig. 6. Stewarton highwall, June 1971.

Lower seam, but Staines (1972) has renamed it the Argo seam. The Argo seam is formed by the union of the Orion and Pollux seams, which are split from each other elsewhere in the Blackwater coalfield (Fig. 30). The Argo seam averages 6.1 m in thickness, and its component seams extend south from the Mackenzie River at least to the southern limit of the outcrop belt of the Rangal Coal Measures (Fig. 2). A zone of fossil logs stratigraphically above the Argo seam occurs on the surface near the seam outcrop and has been useful in tracing the coal. This Report examines the local rather than the regional splits which affect the Argo seam.

The Rangal Coal Measures are interpreted as non-marine. The Lower Triassic Rewan Formation, which conformably overlies the coal measures, was deposited in a fluvial environment. The absence of positive evidence of marine origin in the coal measures, occurrence of freshwater units above and below them, and the low boron content of Blackwater coal (Swaine, 1971) indicate their terrestrial origin. Jensen (1971) identifies the Rangal Coal Measures as the lateral and vertical accretion deposits of a fluvial system; Dickins & Malone (1973) describe them as paludal; and Staines (1972) interprets them as lacustrine.

The palaeocurrent direction in the Burngrove Formation and Rangal Coal Measures was toward the west-northwest (Jensen, 1971). This reflects a reorganization of the drainage pattern after south-southwest-flowing streams deposited the Fair Hill Formation. During deposition of the coal measures, basin subsidence was more rapid than the rate of sediment supply (Jensen, in press).

STRUCTURE

Regional Structure

The Rangal Coal Measures in the Blackwater area lie on the eastern limb of the Comet Ridge and dip gently eastward into the Mimosa Syncline (Fig. 2). Two sets of regional folds affect the Utah Development Company Proclaimed Area. The axial trend of one set corresponds to the northwestern trend of the Folded Zone (Malone, Olgers, & Kirkegaard, 1969), which is northeast of Blackwater. The second set of folds trends northward parallel to the axis of the Mimosa Syncline (King, Goscombe, & Hansen, 1963). Faults commonly trend in complementary northwestward and northeastward directions in the Blackwater area.

Local Structure

Structure of the Argo seam in the mine area

The configuration of the surface upon which the Argo seam peat developed and that of the peat surface itself influenced the depositional and compactional history of the coal measures above the seam. Field observations indicate that neither surface is a simple plane conforming only to the gentle eastward regional dip. Structure contour maps of the bottom and top of the Argo seam show that these surfaces are not necessarily parallel, and have local undulations.

Structure contours on the bottom of the Argo seam clearly illustrate the easterly regional dip (Fig. 7). The dips calculated from Figure 6 agree with values reported by Utah Development Company. The calculated regional dip increases from 3.5° between C4+8 and C4+1 to 4° at C4–5, 5° at C4–11, and 5.5° at C4–13. South of C4–14 the regional dip increases rapidly from 9.5° at C4–16

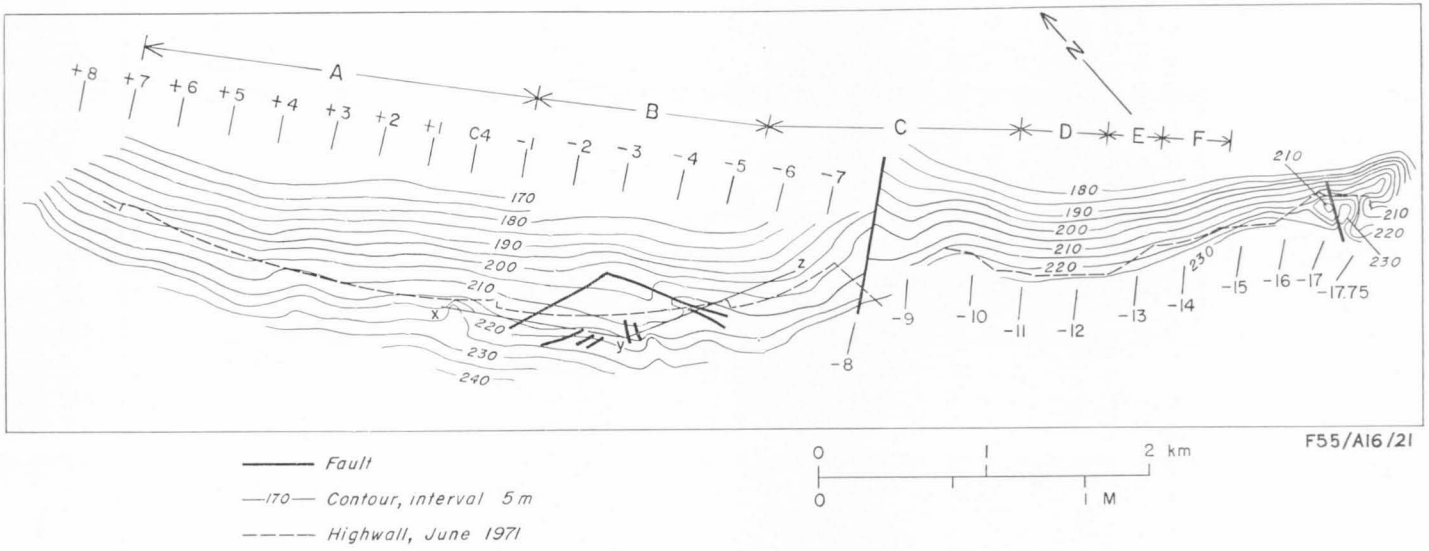

Fig. 7. Structure contours on the bottom of the Argo seam. Contour interval: 5 m.

to 11° at C4 – 16.5 and 12° at C4 – 17.25. Broad gentle folds are superimposed on the regional dip near C4+4, C4 – 3, C4 – 6, C4 – 10, C4 –11, C4 – 13, and C4 – 16. Contour irregularities between C4 – 7 and C4 – 9.5 indicate the presence of a major structure in the unmined area between the Deep Creek/Taurus and Stewarton pits. This structure is probably an east-trending fault along which the southern block moved relatively eastward. A southeast-plunging anticline and adjacent syncline occur south of C4 – 16.5 in the region of greater dip. Near C4 – 17 the anticline is cut by an east-trending fault along which the southern block is upthrown relative to the northern block.

Two local ridges occur in the rocks below the Argo seam in the Deep Creek/Taurus pit (Figs 7, 18). The axis of the short northern ridge roughly coincides with C4. This ridge has a steep northern flank and more gentle southern flank. The southern ridge between C4 – 4 and C4 – 6 is morphologically more complex, with a northern spur along C4 – 4, a southern spur along C4 – 5, and an eastern spur which trends northward near C4 – 5. The locations of the ridges roughly coincide with part of the boundary along which sediments splitting the coal seam pinch out or with areas where they thin. No local ridges are associated with the Stewarton split.

Comparison of structure contour maps of the top (Fig. 8) and bottom (Fig. 7) of the Argo seam shows that the same structural features are apparent on both surfaces, but that the positions and shapes of the two Deep Creek/Taurus local ridges are slightly different on the top surface of the seam. However, as expressed in Figure 18 these local ridges maintain their positions relative to pinch-out and thinning trends of sedimentary rocks in the split. The ridges are not shown on Utah Development Company top-of-coal contour maps. No local irregularities occur on the top surface of the coal at the edges of the Stewarton split (Fig. 8).

The Argo seam is draped over local ridges and broad gentle folds that were probably produced by differential compaction of the underlying sand and mud. Sand is almost incompressible compared with mud. Sandy areas would thus become ridges which reflect the geometry of the sand bodies. Staines' (1972, p. 8) description of the varying thickness of the interval between the lowest seam in the Rangal Coal Measures and the base of the Argo seam supports this hypothesis: 'Thicker intervals are occupied mainly by sandstone, thinner intervals by siltstone and shale.' The sandstone sequences probably stand relatively higher than adjacent, more compacted siltstone and shale sequences and therefore form the cores of anticlines.

Local folds in the coal measures

The following stratigraphic sequence is generally exposed in the highwall of the mine: (1) coal (Argo seam) at the base; (2) lower carbonaceous shale; (3) interbedded mudstone, siltstone, and sandstone; (4) upper carbonaceous shale: (5) interbedded mudstone, siltstone, and sandstone (Fig. 5, C; Fig. 6, C, E). Interbedded mudstone, siltstone, and sandstone directly overlie the coal seam where the lower and upper carbonaceous shales are absent (Fig. 5, A).

The lower carbonaceous shale is split from the coal by two lenses of mudstone, siltstone, and sandstone. The rocks in the lenses are identical with those which overlie the lower carbonaceous shale. The Deep Creek/Taurus lens reaches a thickness of 28 m in the highwall (Fig. 5, B) and is much larger than the 8 m-thick

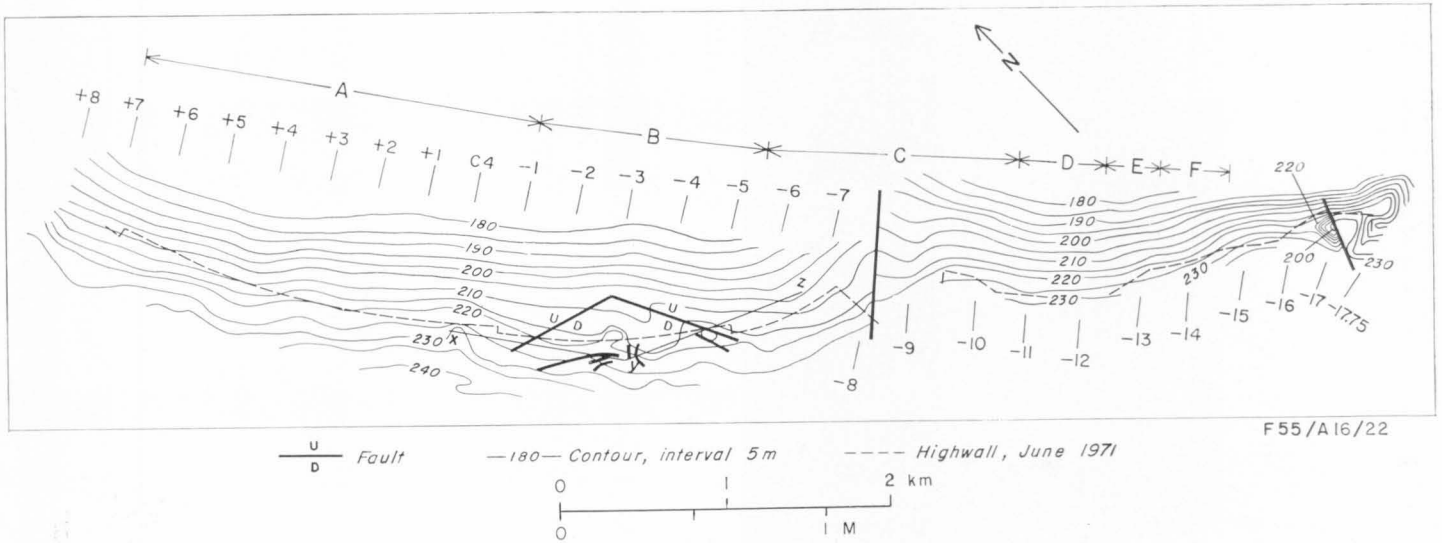

Fig. 8. Structure contours on the top of the Argo seam. Contour interval: 5 m.

Fig. 9A. Southern end of Deep Creek/Taurus split, looking south at highwall from B4 to B9 (Fig. 5).

Stewarton lens (Fig. 6, D). Bedding planes in the lenses form anticlines which are concordant with the overlying lower carbonaceous shale but discordant with the underlying coal seam (Figs 5, B; 6, D; 9 to 12). Beds within the lenses wedge out against the coal seam (Fig. 9).

Adjacent broad folds occur in the interbedded mudstone, siltstone, and sandstone which overlie the lower carbonaceous shale (Figs 5, B5 to B9; 6, C, F; 9; 10; 20). Bedding planes in the structures are discordant with the underlying lower carbonaceous shale, and beds in anticlines wedge out against it (Figs 5, B4 to B9; 9; 10). The upper carbonaceous shale is generally concordant with bedding in rocks above the lower carbonaceous shale (Fig. 6, C to E). Folds identical with those above the lower carbonaceous shale to the south discordantly overlie the coal seam in highwall sections A and B1 to B3 (Rigs 5, 21) where the lower and upper carbonaceous shales are absent.

Interbedded mudstone, siltstone, and sandstone overlie the upper carbonaceous shale in the southern end of the Deep Creek/Taurus pit and in the Stewarton pit (Figs 5, B, C; 6, C, D, E). Clastic rocks above the upper carbonaceous shale are concordant with it, whereas similar rocks above the coal seam and lower carbonaceous shale are discordant with them.

Origin of the Local Folds

The Argo seam is not folded in sympathy with the anticlines and synclines in the rocks which overlie it. In addition, these structures are associated with an

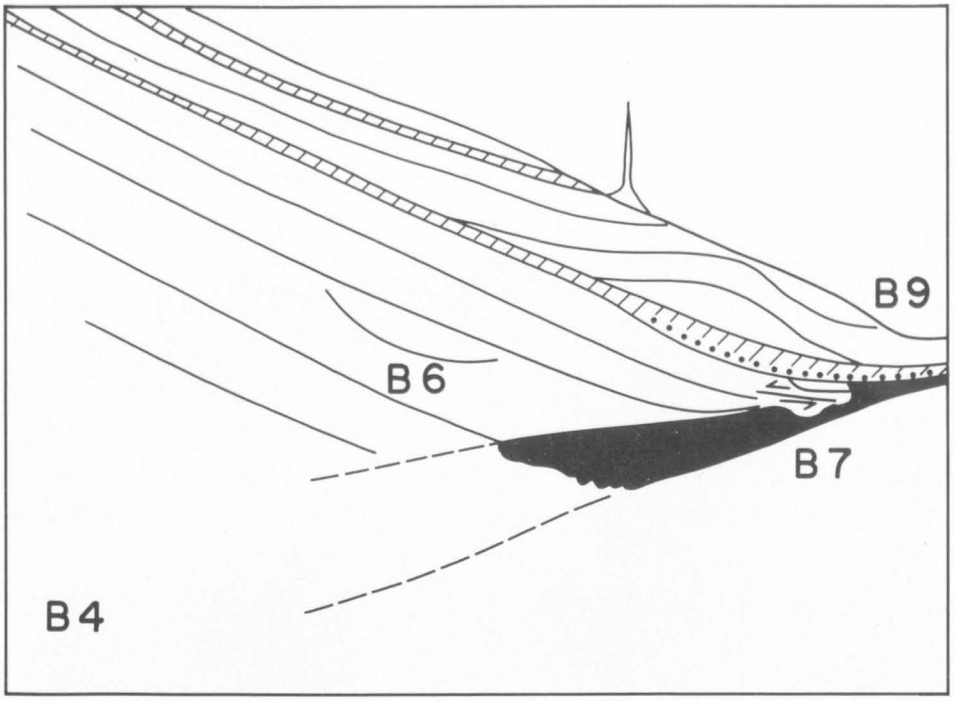

Fig. 9B. Sketch of Figure 9A. Coal (black) overlain discordantly by anticlinal lens between B4 and B7. Beds in lens wedge out against seam, but are concordant with overlying lower carbonaceous shale (diagonal ruling). Cut-and-fill structure in lens (B6). Upper tonstein (dotted line) in lower carbonaceous shale. Folded clastic rocks discordantly overlie lower carbonaceous shale. Upper carbonaceous shale (diagonal ruling) concordant with underlying folded unit. Thrust-faults affect coal and lower carbonaceous shale at split edge (B7).

originally thick accumulation of peat. For these reasons development of the folds above the coal at Blackwater is attributed to deformation during deposition and differential compaction of the sedimentary column rather than to regional tectonic forces.

A generalized model for the development of the seam splits and overlying folds is presented in the following sections. Operation of the mechanisms involved in the model is based upon these principles: (1) vegetable material will become compacted much more than clastic sediment; (2) some areas in a peat deposit may be compacted more rapidly than others; (3) centres of more rapid peat compaction may become relocated with time; (4) carbonaceous mud would not have been deposited on the steep slopes which are now the flanks of the splits and was therefore laid down in essentially horizontal beds; and (5) beds concordant with the lower and upper carbonaceous shales were also deposited horizontally.

The model for development of folds at Blackwater is based upon the same principles and compactional mechanisms as the model Britten (1972) formulated to explain seam splits in the Singleton Coal Measures. The model presented here differs from Britten's by emphasizing the probable role of topographic relief below peat seams in initiating the development of a seam split.

Fig. 10A. Southern end of Deep Creek/Taurus split, looking north at highwall from B9 to B4 (Fig. 5).

Deep Creek/Taurus split model

A thick section of peat being compacted under its own weight accumulated over two local ridges shown by structure contour maps of the Argo seam (Fig. 14a). The peat became compacted at a uniform rate across the area, and its surface reflected the underlying topography as a slight depression developed over the sag between the underlying ridges. This surface depression began to fill with horizontal beds of clastic sediment (Fig. 14b) which will be referred to as first-generation sediments.

Loading by the clastic lens in the surface depression caused non-uniform compaction of peat; peat below the depression became compacted more rapidly than peat in adjacent areas (Fig. 15a). As the depression continued to subside more rapidly than the rest of the peat surface, more horizontal clastic beds were deposited in it. This increased load caused even more rapid subsidence in the depression (Fig. 15b). The load on the edges of the depression increased, and the depression widened as well as deepened. The oldest beds in the depression were warped downward.

As the peat below the depression became more compacted, the rate of compaction decreased, and the depression filled with clastic sediment. Peat adjacent to the depression retained greater compactional potential than peat below the depression. Consequently, subsidence became relatively more rapid adjacent to the depression than below it. The lens of first-generation sediments filling the depres-

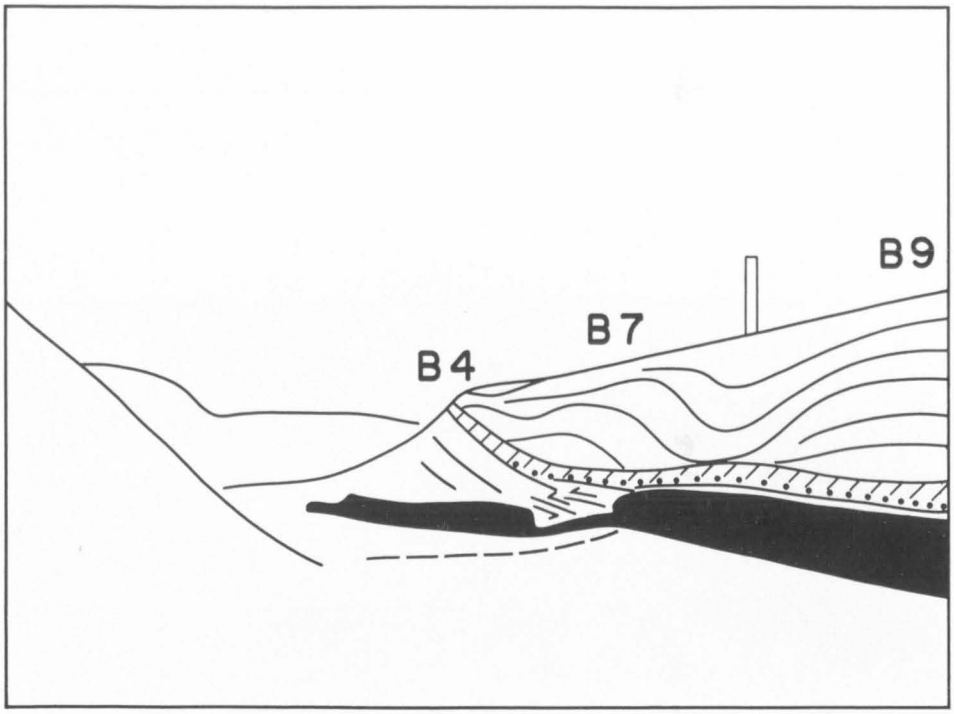

Fig. 10B. Sketch of Figure 10A. Coal (black) over anticline (axis shown by dashed line) in underlying rocks. Lower carbonaceous shale (diagonal ruling) split from coal by anticlinal lens between B4 and B7 and by thin bed of carbonaceous sandstone between B7 and B9. Upper tonstein shown by dotted line. Broad adjacent folds discordantly overlie and wedge out against lower carbonaceous shale.

sion was almost incompressible relative to peat. Because of this and the slower rate of peat compaction below the depression, the lens of sediments became slightly higher relative to the peat surface. Carbonaceous mud was deposited over the peat and lens (Fig. 16a).

As the peat adjacent to the original depression continued to be compacted more rapidly, the relief increased (Fig. 16b). Beds warped downward during filling of the depression were flattened out, and horizontal beds in the first-generation lens were bowed upward. A second generation of depressions developed on the flanks of the first-generation mound, and horizontal beds of second-generation clastic sediment were deposited in them. Loading in depositional areas further increased the already more rapid rate of peat compaction below the second-generation depressions. Deposition eventually buried the first-generation lens. The carbonaceous mud became compacted, and clastic beds overlying it were draped over the ridges below the peat to produce discordant folds above and alongside the first-generation lens (Fig. 17). A second carbonaceous mud was deposited over the second-generation clastic sediments before or as they were folded (Figs 5, B, C; 6, C, D, E).

When the second-generation depressions were full, the general rate of subsidence in the area was slower because the peat was already considerably compacted. However, second-generation lenses of clastic sediment evolved into mounds

Fig. 11A. Northern end of Deep Creek/Taurus split, looking north at highwall from B2 to A6 (Fig. 5).

above the surface of the second carbonaceous mud (Figs 5, B, C; 6, C, E) by differential compaction in a manner analogous to growth of the first-generation mounds; the rate of peat compaction became relatively more rapid below the first-generation lens than below the second generation lenses. Second-generation mounds were separated by third-generation depressions in which horizontal beds of clastic sediment were deposited. The third-generation depressions were roughly located above the first-generation mounds (Figs 5, B; 6, C, D, E).

A profile of coal thickness along cross-section XYZ (Figs 18, 19) permits more detailed reconstruction of the development of the Deep Creek/Taurus split. The profile is derived from an isopach map of the Argo seam plotted by computer Fig. 19). The coal thins over the southern local ridge at C4 – C5. This indicates that the ridge formed before or during early stages of peat accumulation. Small-displacement thrust-faults repeat the coal at C4 – 5, so some of the increase in coal thickness immediately south of C4 – 5 may be caused by faulting. The Argo seam varies little in thickness between C4 and C4 – 5. The coal thickens slightly rather than thinning over the northern local ridge at C4 (Figs 18, 19), suggesting that the ridge grew during late stages of or after peat accumulation. It did not affect the amount of peat accumulated, but as it formed it affected the configuration of the peat surface above it. This northern ridge may have been produced by differential compaction of sand and mud below the Argo seam.

Stewarton split model

Once the first-generation depression had formed, the Stewarton split (Fig. 6, D1 to E2) evolved in the same way as the Deep Creek/Taurus split. Structure

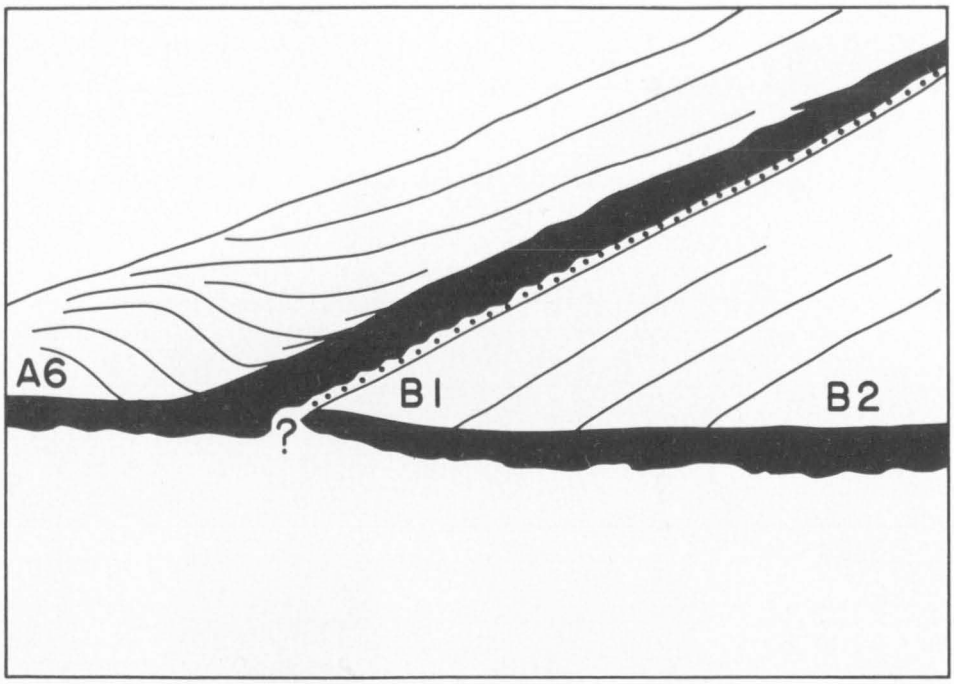

Fig. 11B. Sketch of Figure 11A. Anticlinal lens (B1 to B2) splits shaly coal (black) from coal seam (black). Bedding in lens concordant with shaly coal but discordant with underlying seam. Rocks above seam and shaly coal are folded and dip discordantly onto them (A6 to B2). Upper tonstein (dotted line) in shaly coal.

contour maps of the Argo seam show that the Stewarton split overlies a syncline in the coal between two broad gentle anticlines (Figs 7, 8). No local ridges of the Deep Creek/Taurus type are associated with the Stewarton split. The coal seam does not vary in thickness over the anticlines or beneath the split. The anticlines must therefore have formed during late stages of or after peat accumulation; differential compaction of sand and mud under the load of peat may have caused growth of the structures. If the anticlines were growing as first-generation sediments were being deposited, their formation may have triggered development of the first-generation depression in the peat surface. If the anticlines are younger structures, non-uniform compaction of peat must have been responsible for initial development of the first-generation depression, below which compaction was relatively rapid. The first-generation lens and mound (Fig. 6, D), second-generation lenses and mounds (Fig. 6, C, E), and third-generation lens (Fig. 6, C, D) developed in the same manner in the Stewarton split as in the Deep Creek/Taurus split (Fig. 5, B). The absence of local ridges below the edges of the Stewarton split (Figs 7, 8) may explain the relative structural simplicity of second-generation sedimentary rocks closely associated with it (Fig. 6, C5, E2).

Major folds in second-generation sedimentary rocks

Second-generation clastic sediments lie in large folds discordant with underlying carbonaceous beds far from as well as near first-generation lenses. Development of the more distant folds was not directly controlled by growth of first-genera-

Fig. 12A. Northern end of Deep Creek/Taurus split, looking south at highwall from A6 to B3 (Fig. 5).

tion mounds, but rather by conditions within the second-generation depressions themselves.

Folded clastic rocks above the Argo seam north of B1 (Fig. 5) are identified as second-generation sedimentary rocks because they overlie the shaly coal which was deposited over the first-generation lens between B1 and B3. As the first-generation mound formed, a second-generation depression extended northward from B1 at least to A1. A large syncline in the second-generation sedimentary rocks overlies an anticline in the Argo seam from A3 to A5 (Figs 5, 21). Beds adjacent to the syncline lie in very broad anticlines which dip onto the coal (Fig. 5, A1 to A4, A5 to A7). The Argo seam does not thin over the anticline in the coal (Fig. 22); this structure formed during late stages of or after peat accumulation. Erosional structures on the surface of the anticline (p. 23) suggests that it was probably growing as the second-generation depression began to fill with sediment. This anticline also may be a product of differential compaction of sand and mud below the peat. The growing structure became a slight mound in the second-generation depression, and depositional areas were subdivided into smaller depressions in which the oldest second-generation sediments were laid down. Loading in the smaller depressions caused the peat below them to be compacted more rapidly than that overlying the growing anticline. Sedimentation continued in the small depressions. Eventually, growth of the anticline slowed, and the greater compactional potential of peat over the anticline quickened subsidence there. Consequently, relatively incompressible sediments in the smaller depressions became slight anticlinal mounds in the second-

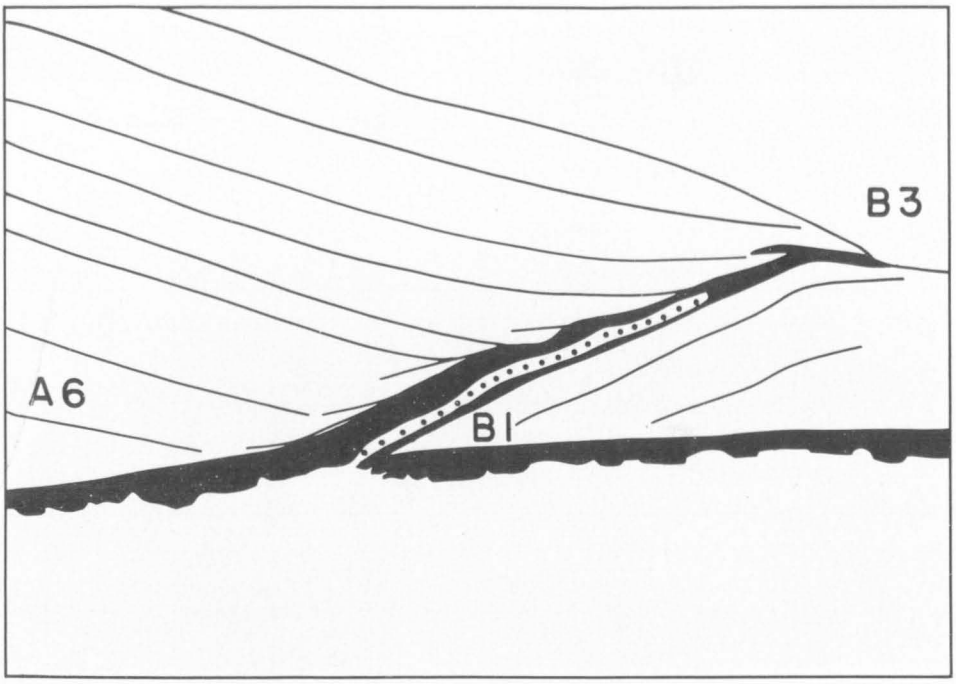

Fig. 12B. Sketch of Figure 12A. Anticlinal lens (B1 to B3) splits shaly coal (black) containing upper tonstein (dotted line) from coal seam (black). Bedding in lens concordant with shaly coal but discordant with seam. Rocks above shaly coal concordant with it and coal seam. 'Fish-tails' in upper surface of shaly coal.

generation depression, now characterized by anticlinal structures. Second-generation sediments then filled a smaller depression over the anticline in the coal between the mounds to produce the syncline between A4 and A5 (Fig. 5).

The growth of two anticlines below the Argo seam peat may explain the formation of an anticline in second-generation sediments above the lower carbonaceous shale in section F of the Stewarton highwall (Figs 6, 20). The axis of a broad gentle syncline in the coal trends east-northeast at C4 – 13.5 (Fig. 8) between two anticlines. The anticline in second-generation sedimentary rocks lies above the syncline in the coal. The Argo seams vary little in thicknesses across the anticlines in it; therefore the anticlines grew during late stages of or after the accumulation of the peat. As in the Deep Creek/Taurus area, the growing anticlines subdivided the second-generation depression (E1 at least to F3) into small depressions, one of which (F1 to F3) lay between the slight mounds. This small depression filled and evolved into an anticline by differential compaction. Elevation of a first-generation lens south of F3 (Fig. 38, C4 – 14 to C4 – 17.5) probably occurred before deposition in second-generation depressions (p. 48) and may have influenced development of the anticline.

Compactional and depositional mechanisms responsible for the gross morphology of first and second-generation lenses also produced similar structures within those lenses.

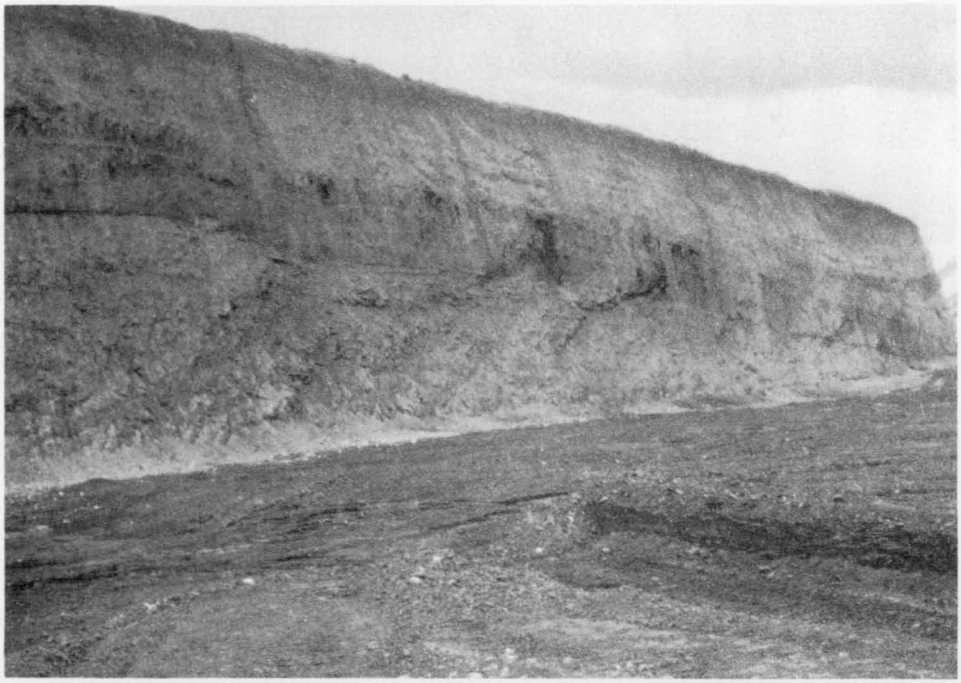

Fig. 13A. Southern end of the Stewarton split, looking south at highwall from D2 to E1 (Fig. 6).

Faulting and Sedimentary Intrusions

Compactional adjustments of the sedimentary column are expressed not only as folds but also as small-displacement faults, stone rolls, and stone intrusions into the coal seam. The faults commonly record differential movement of the coal and lower carbonaceous shale.

Utah Development Company maps show a long fault between C4 – 1 and C4 – 5.5 (Fig. 8). The fault runs roughly parallel to the eastern edge of the Deep Creek/Taurus split (Fig. 38) and cuts that body. The western block, where sediments within the split are more voluminous, is downthrown relative to the eastern block. The vertical displacement along the fault is 3 m at its northern and southern ends and increases to 6 to 9 m between C4 – 3 and C4 – 4. This fault was observed to be a low-angle thrust where it intersects the highwall at C4 – 5 (Figs 5, B7; 9; 10) and C4 – 5.5 (Fig. 23). At both places the upper part of the coal, sedimentary rocks within the split, and basal section of the lower carbonaceous shale are repeated twice. The upper part of the lower carbonaceous shale and rocks above it are undisturbed. Motion along the fault is interpreted as compactional adjustment which allowed the western block, more heavily loaded with first-generation sediments, to sink relative to the eastern block. Movement at least postdated deposition of the basal part of the lower carbonaceous shale; it may have occurred as the first-generation clastic lens became a mound. Other small faults cause brecciation in the coal seam below the split (Figs 8, 38).

Floor rolls of first-generation clastic sediments project upward into the base of the lower carbonaceous shale at D1 and D3 (Fig. 6) in the Stewarton pit.

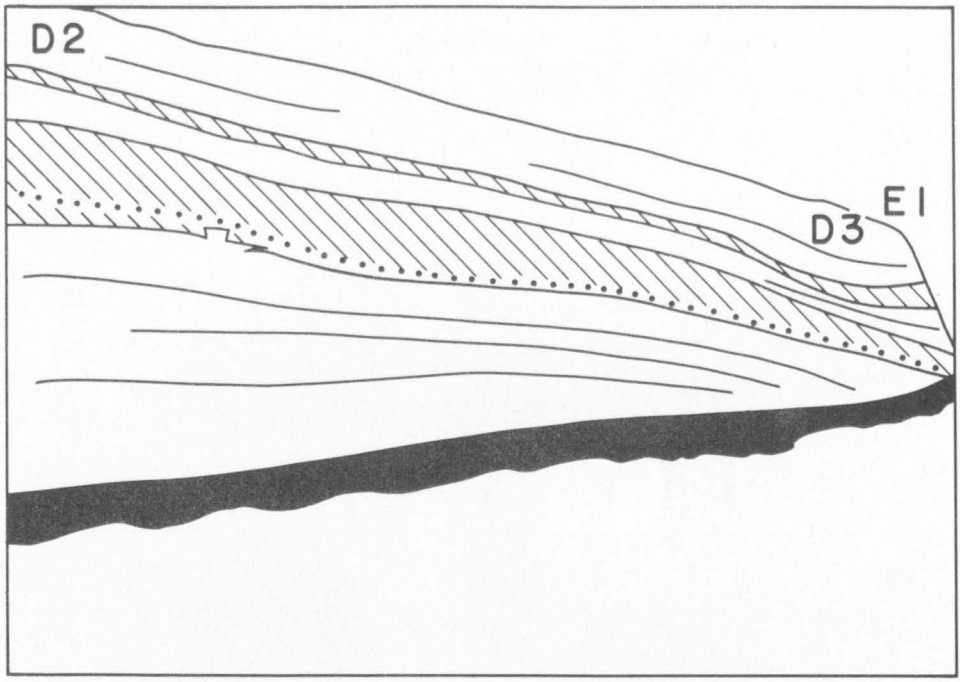

Fig. 13B. Sketch of Figure 13A. Lower carbonaceous shale (diagonal ruling) containing upper tonstein (dotted line) split from coal seam (black) by anticlinal lens (D2 to E1). Bedding in lens concordant with lower carbonaceous shale but discordant with coal seam. Upper carbonaceous shale (diagonal ruling) diverges from lower carbonaceous shale at D3.

Development of these structures and of the disturbed bedding which accompanies them is attributed to compaction after deposition of the lower carbonaceous shale. Minor compaction faults cut the two carbonaceous shales at D2.

Roof rolls of second-generation sediments occur in the top of carbonaceous layers below synclines at two places in the Deep Creek/Taurus pit. From A3 to A5 the rolls are in the top of the Argo seam (Figs 5, 21); at B8 (Figs 5, 24, 25) they lie in the top of the lower carbonaceous shale. Williamson (1967) attributes formation of roof rolls to local erosion of the peat surface soon after peat deposition or to loadcasting. 'Fish-tails' (thin stringers of coal: Raistrick & Marshall, 1939, pp. 81-83) extend into second-generation sedimentary rocks from the shaly coal which overlies the Deep Creek/Taurus first-generation lens (Figs 5, B1, B3; 11). 'Fish-tails' develop where erosion cuts into peat and causes individual layers to splay out along bedding planes (Williamson, 1967). According to the model presented here, the Deep Creek/Taurus first-generation lens stood as a mound during deposition in second-generation depressions; the synclines at A4—A5 and B8 (Fig. 5) are underlain by anticlines in the coal, which stood as lower mounds within the second-generation depressions. Local erosion on the flanks of the mounds before they were buried by deposition may have produced the roof rolls and 'fish-tails'. Complex sandstone intrusions are associated with roof rolls and 'fish-tails' at B8 (Figs 24, 25). The intrusions are interpreted as compaction features related to local erosion of the lower carbonaceous shale.

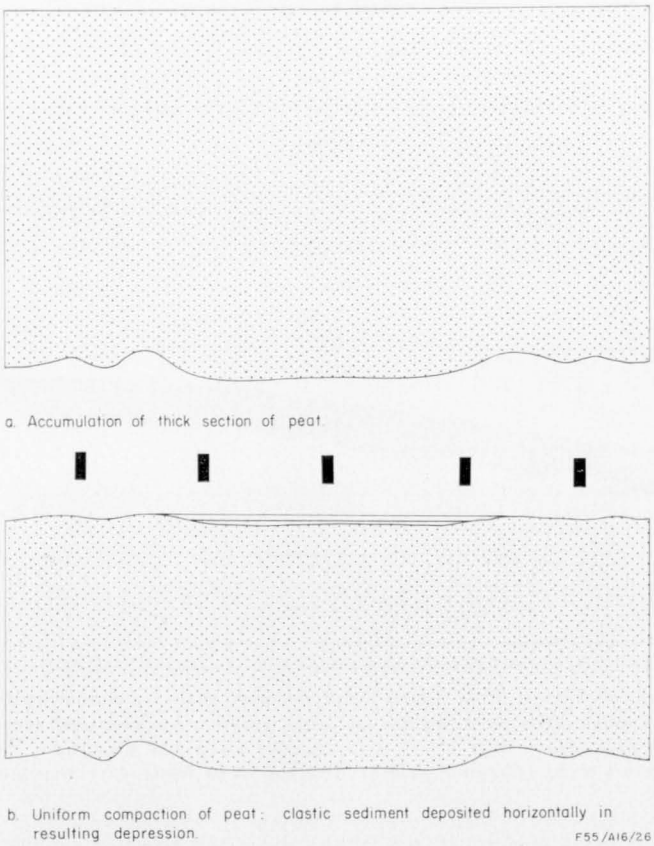

Fig. 14. Initial stages in the development of a split. The bars above the cross-section are proportional to the rate of subsidence at various localities.

High-angle thrust and normal faults cut most or all units exposed in the highwall at various localities (Figs 5, A1, A2, A8; 6, C3, E3, F1). They may be tectonic rather than compactional structures.

Controls of Split Development

First, second, and third-generation folds constitute a complex genetic unit and were produced by (1) variable rates of peat compaction at different places at one time; (2) variable rates of peat compaction at one place through time; and (3) the virtual incompressibility of clastic sediments relative to peat. Depositional and compactional mechanisms combined to produce a dynamic, mobile sedimentary sequence.

The mechanism which triggered development of first-generation depressions is incompletely understood. Non-uniform compaction of peat caused by local conditions within the peat itself could have initiated formation of rapidly subsiding depressions. This mechanism does not, however, account for the general association of anticlinal ridges below and in the coal seam with the edges of first-generation lenses. Uniform compaction of peat over neighbouring ridges which existed before

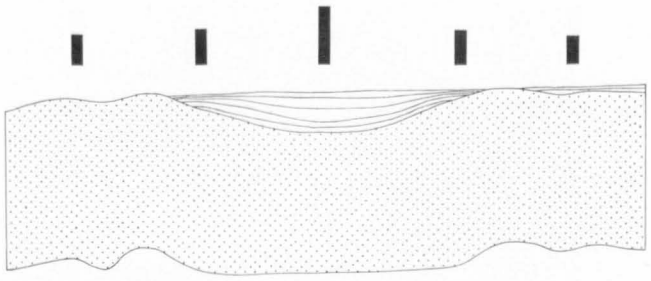

a. Non-uniform compaction of peat: loading by clastic lens causes more rapid subsidence in depression; deposition of horizontal clastic beds continues; oldest beds warped downward.

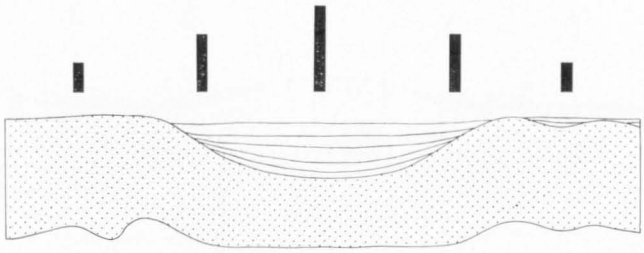

b. Non-uniform compaction of peat: continuation of a. F55/A16/27

Fig. 15. Intermediate stages in the development of a split. The bars above the cross-sections are proportional to the rate of subsidence at various localities.

peat accumulation can explain this association and development of first-generation depressions. In this case the peat would be thinner over anticlinal ridges than in adjacent depressions. The Argo seam thins only over the ridge at the southern end of the Deep Creek/Taurus split, and therefore another mechanism must also have operated to produce first-generation depressions. The growth of anticlines caused by differential compaction of sand and mud bodies below the peat may have been such a trigger. The general uniformity of coal thickness over anticlines indicates that these structures began to grow during late stages of or after peat accumulation; a heavy load of peat may have been necessary to produce compaction in underlying sediments. First-generation depressions may have formed and begun to fill as the anticlines grew. Compactional growth of anticlines may also be responsible for subdivision of second-generation depressions. The compactional origin of the anticlines and synclines superimposed on the regional dip of the coal must, however, remain a hypothesis. Although sandy intervals are known to be thicker than muddy intervals in the coal measures below the Argo seam (Staines, 1972), exact facies distributions below the seam are too poorly known to eliminate the possibility of later tectonic origin for the structures.

Folds above the Argo seam are compactional structures which may develop wherever depressions form as the result of peat compaction over pre-existing

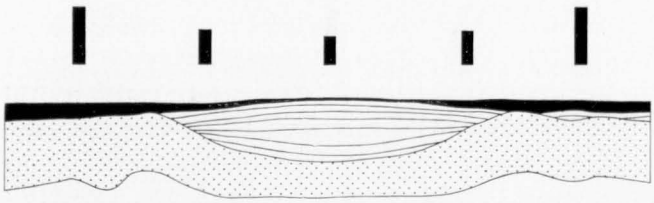

a. Non-uniform compaction of peat: greater compactional potential of peat flanking depression causes more rapid subsidence there; relatively incompressible clastic lens becomes slight mound; deposition of carbonaceous mud.

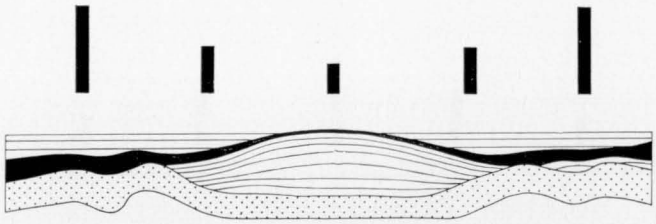

b. Non-uniform compaction of peat: continuation of a. with deposition of horizontal clastic beds on flanks of mound; loading increases rate of subsidence in depositional areas; folding of first-generation sediments. F55/A16/28

Fig. 16. Late stages in the development of a split. The bars above the cross-sections are proportional to the rate of subsidence at various localities.

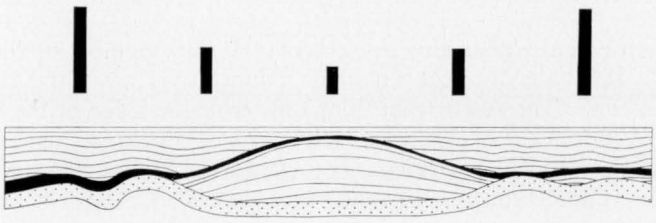

Non-uniform compaction of peat: deposition buries clastic lens; compaction of carbonaceous mud; compactional deformation of flanking beds. F55/A16/29

Fig. 17. Final stage in the development of a split. The bars above the cross-section are proportional to the rate of subsidence at various localities.

irregularities or over growing anticlines. The folds may develop in any depositional environment in which those conditions exist, and therefore the structures themselves as seen in two dimensions in the mine highwall have no specific environmetal significance. However, the nature of the sediments filling the depressions and the three-dimensional geometry of the seam splits provide data which identify the depositional environment in which the structures formed at Blackwater.

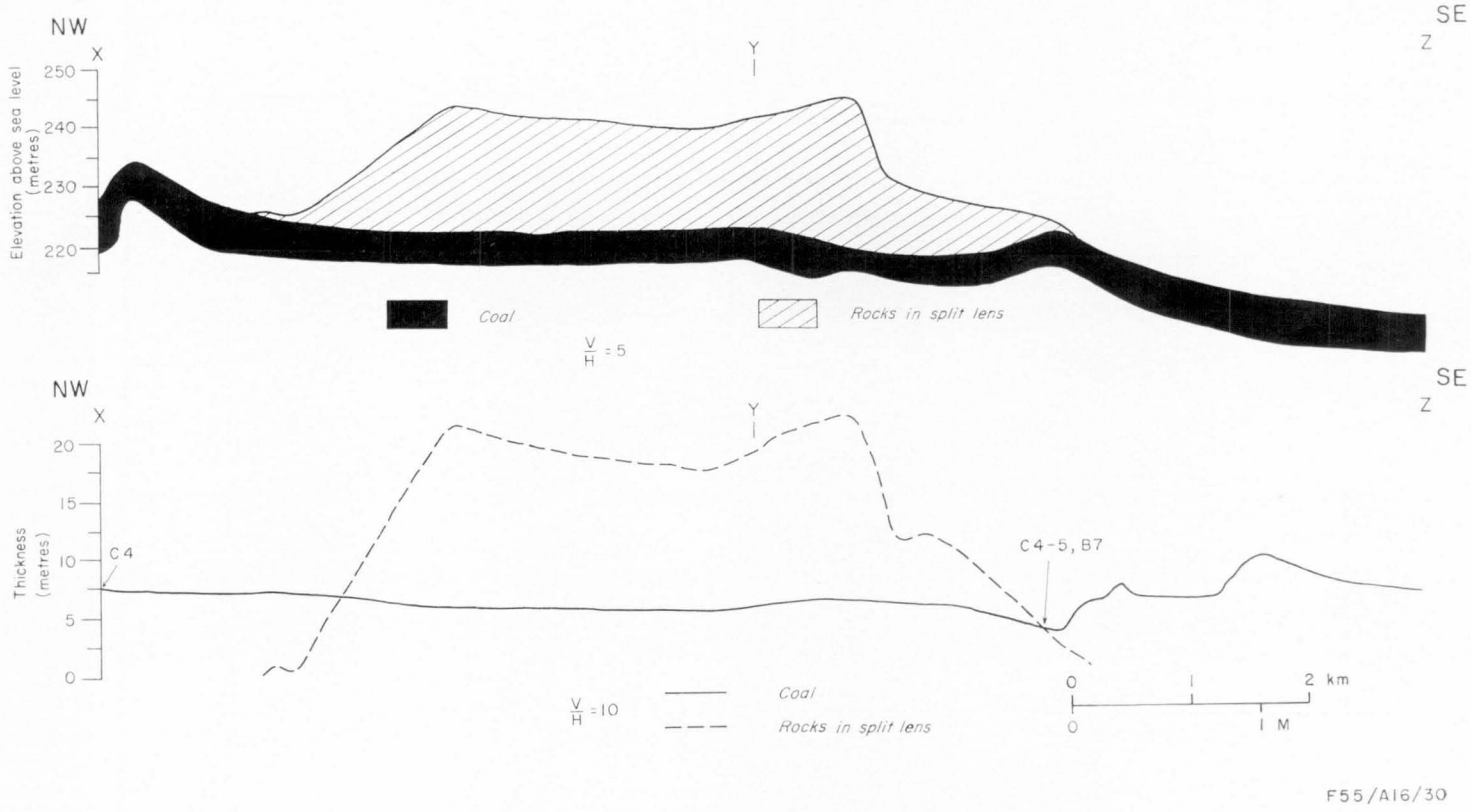

Fig. 18. Cross-section of Deep Creek/Taurus split. Horizontal scale = 1:4800.

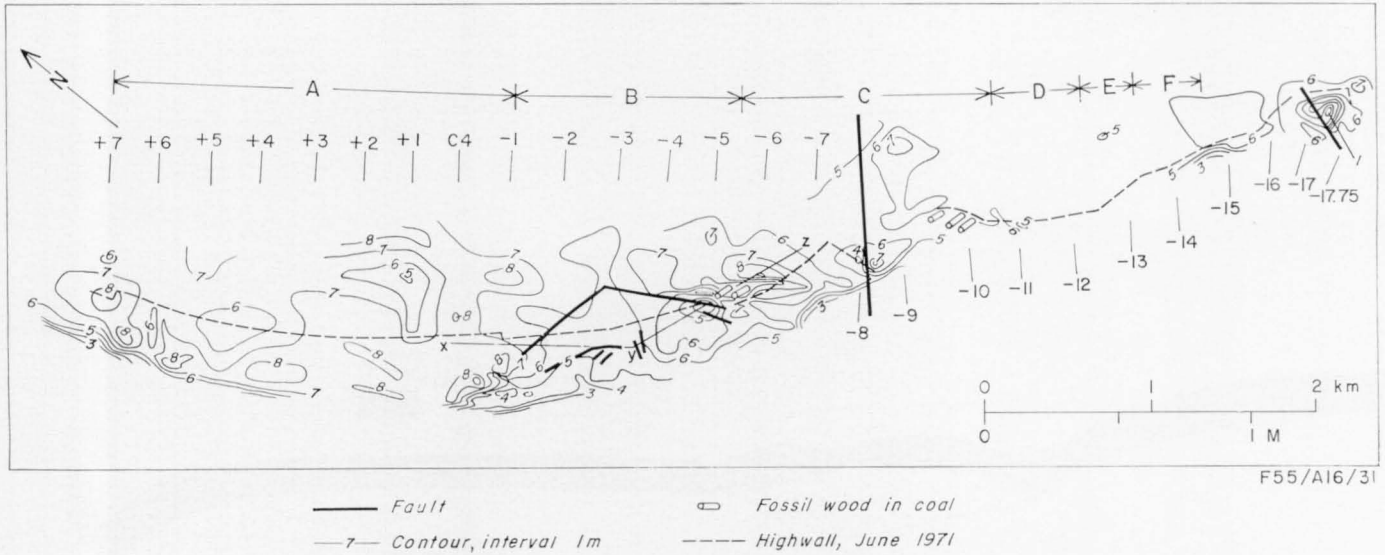

Fig. 19. Isopach map of the Argo seam. Contour interval: 1 m.

Fig. 20. Anticline in sandstone discordantly overlies coal and lower carbonaceous shale, highwall section F (Fig. 6).

THE VERTICAL PROFILE: DEPOSITIONAL ENVIRONMENTS OF UNITS IN THE MINE

Lower Sandstone

The lowest unit exposed in the mine is a sandstone referred to in Utah Development Company reports as the basal 'Sugarloaf Member' of the Rangal Coal Measures (King, Goscombe, & Hansen, 1963). Hansen (1965) describes the 'Sugarloaf Member' as 30 m of medium-grained feldspathic lithic sandstone which contains minor coal seams and beds of carbonaceous shale. Because of its stratigraphic position in the mine and lack of formal definition, the 'Sugarloaf Member' will here be informally called the lower sandstone. The upper 1 to 4 m of the lower sandstone is exposed in the walls of vehicle ramps 1, 2, and 5 (Fig. 3). Four metres of sandstone at an unknown depth lower in this unit is exposed in a drainage ditch just east of and parallel to the haul road between C4 – 9 and C4 – 13. The lower sandstone is not exposed in the highwall, but some company drill holes penetrated the top of the unit. Their distribution shows that the lower sandstone occurs throughout the mine area and in places directly underlies the Argo Seam.

The lower sandstone is light grey to buff, fine to medium-grained, and characterized by large-scale trough cross-stratification (Fig. 28). Bedding characteristics are summarized in Appendix 1. Parallel and ripple-drift laminated sand-

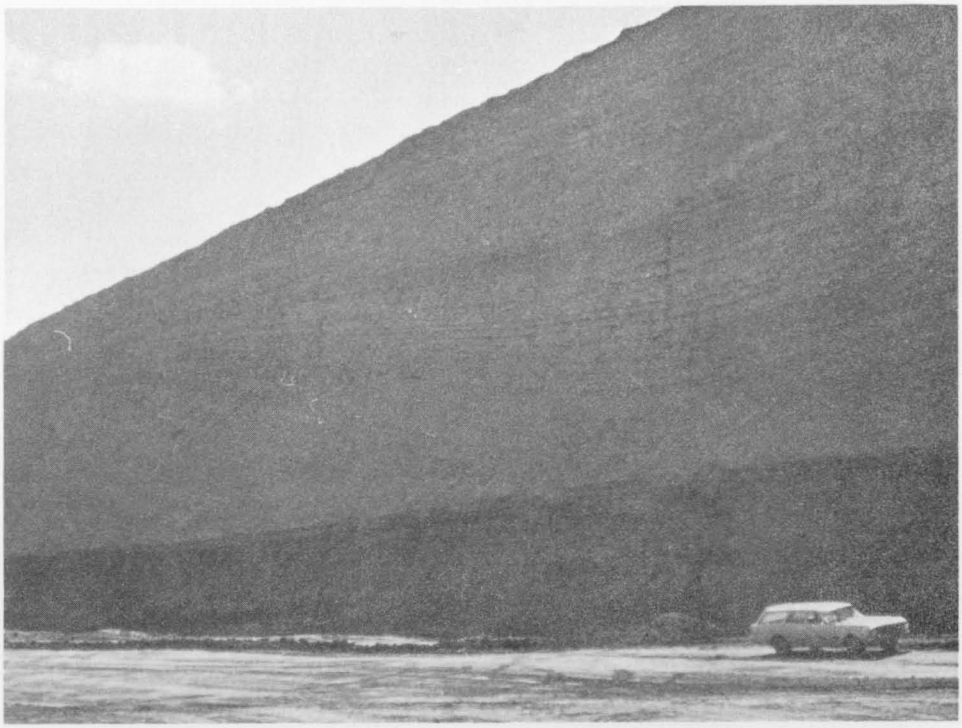

Fig. 21. Syncline in clastic rocks discordantly overlies coal, highwall from A2 to A5 (Fig. 5). Roof rolls and 'fish-tails' at top of seam below synclinal axis.

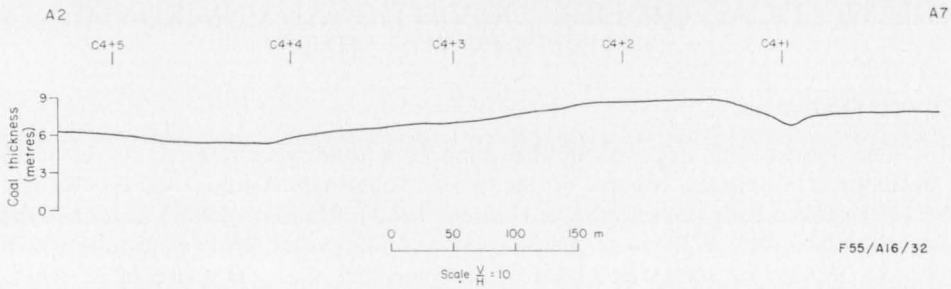

Fig. 22. Coal thickness, Deep Creek/Taurus highwall, A2 to A7 (Fig. 5). Scale $\frac{V}{H} = 10$.

stone, laminated siltstone, and mudstone are thinly interbedded with the cross-stratified sandstone. Fossil wood and flecks of carbonaceous material are abundant in some beds. A unit of very fine-grained sandstone 2 m thick lies between beds of fine-grained cross-stratified sandstone in the ditch section. The very fine sandstone contains plant fragments and rare lenses of cross-stratified fine-grained sandstone.

The orientations of 144 cross-strata measured on ramps 1 and 5 and in the drainage ditch show that the palaeocurrents which deposited the lower sandstone flowed to the west-northwest (Fig. 26). These data confirm palaeocurrent direc-

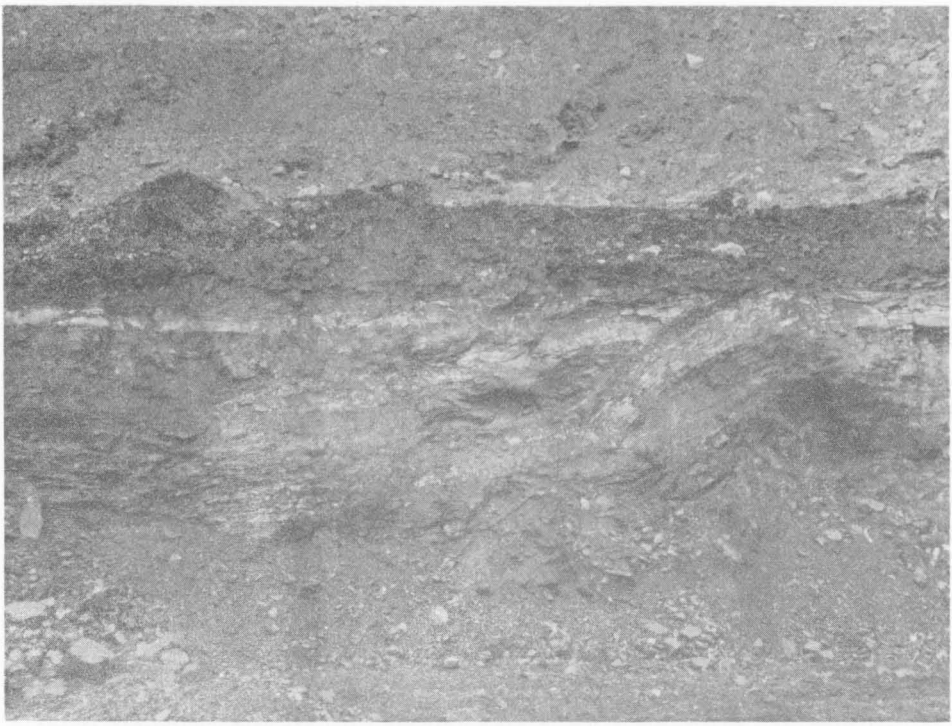

Fig. 23. Double thrust-fault cutting approximately 3 m of coal, sandstone which splits coal and carbonaceous shale, and lower carbonaceous shale at the intersection of a crosswall and the highwall at C4—5.5 (Fig. 8). Coal brecciated and contorted, upper part of lower carbonaceous shale undisturbed.

tions determined by Jensen (1971). Bearings on the long axes of 16 fossil logs in the lower sandstone show a preferred east-northeast orientation which forms an oblique angle with the palaeocurrent direction determined from cross-strata. Fossil wood orientations parallel, perpendicular, and oblique to fluvial flow direction have been reported (Potter & Pettijohn, 1963; Brunt, 1969). Pelletier (1958) suggests that the perpendicular wood orientation is caused by the lodgement of fragments in troughs in the lee of bedforms. The oblique orientation of fossil logs in the lower sandstone may be attributed to the combined effects of current direction and river-bottom geometry at the time the water-saturated wood was deposited.

The lower sandstone is interpreted as a point-bar deposit (Fig. 43). The grainsize of the lower sandstone, together with its thin siltstone interbeds, large and small-scale cross-stratification, and drifted plant remains are typical of point-bar sediments (Allen, 1965a). The position of the sandstone below a grey mudstone unit places it in a sequence fining upwards, the vertical profile produced by lateral migration of a meandering river channel (Allen, 1965b).

Grey Mudstone

A thin unit of grey mudstone* and siltstone overlies the lower sandstone and is exposed on vehicle ramps 1, 2, and 5 (Fig. 3). Company drill-hole data prove

* In this Report the term mudstone refers to laminated and non-laminated rocks composed of clay and silt-sized particles.

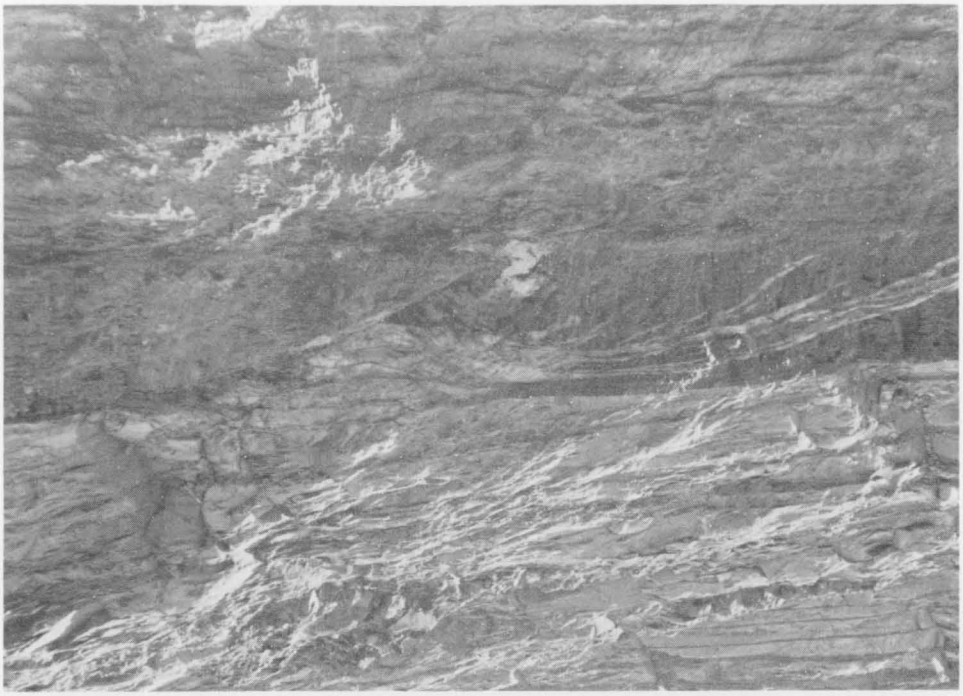

Fig. 24. Roof roll approximately 0.5 m thick, 'fish-tail', and sandstone intrusions in top of lower carbonaceous shale, highwall section B8 (Fig. 5). Overlying clastic rocks dip onto and wedge out against lower carbonaceous shale .

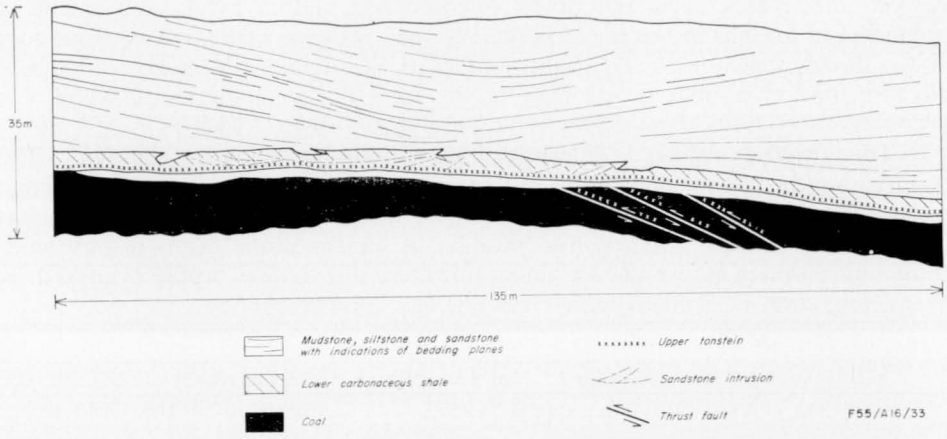

Fig. 25. Detailed highwall map, Deep Creek/Taurus section B8 (Fig. 5).

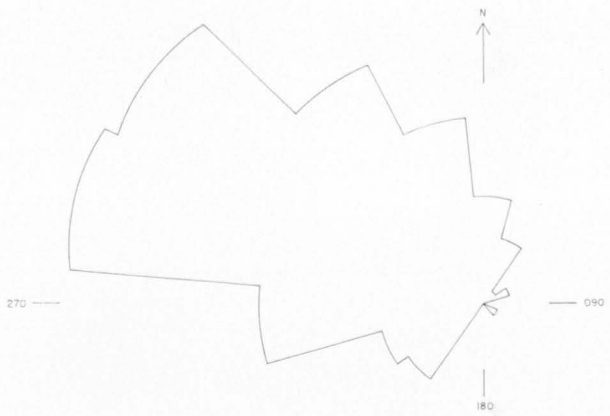

Fig. 26. Orientation of cross-strata in lower sandstone (ditch, ramp 1, and ramp 5); 144 measurements.

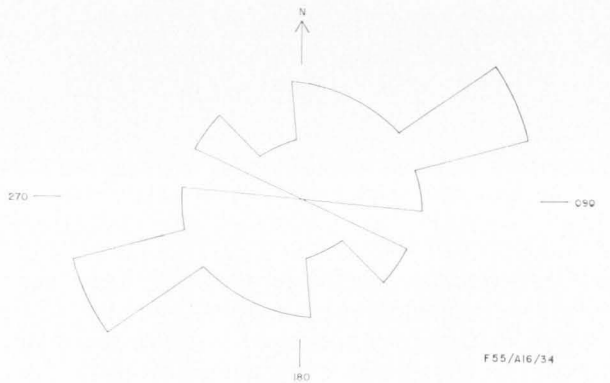

Fig. 27. Orientation of fossil wood long axes in lower sandstone (ditch and ramp 5); 16 measurements.

that this mudstone directly underlies the Argo seam throughout much of the mine area and reaches a thickness of at least 4.5 m. It is locally absent and thickens away from areas where the lower sandstone directly underlies the Argo seam. The grey mudstone was probably deposited around but not over elevated areas on the sandstone surface.

The grey mudstone unit is 2.3 m thick on ramp 5 (Fig. 28). The basal 0.3 m consists of interbedded grey mudstone and very fine and fine-grained buff sandstone and represents a transition from the lower sandstone to the grey mudstone. The main body of the mudstone unit consists of 1.4 m of laminated grey mudstone and siltstone with rare buff sandstone interbeds. The top 0.6 m of the unit is composed of interbedded grey mudstone, coal, and black carbonaceous shale and marks a gradual transition to the Argo seam.

Fig. 28. Cross-stratified lower sandstone overlain by grey mudstone and oxidized coal (black) of the Argo seam, south wall of vehicle ramp 5 (Fig. 3).

Fossil roots and leaves are abundant in the grey mudstone unit. Well preserved whole leaves are very common just below the Argo seam near B6 (Fig. 5). *Vertebraria* is present throughout the grey mudstone on ramps 1, 2, and 5 (Fig. 3). White (1969) reports that study of specimens in which tissue structures are well preserved has proved that *Vertebraria* is a gymnosperm root.

The grey mudstone unit is interpreted as an overbank deposit laid down during river floods (Fig. 43). It is characterized by a finer grainsize than the underlying lower sandstone, lamination, roots, and drifted leaves. These features are typical of overbank sediments (Allen, 1965a). The presence of vertical roots in the grey mudstone indicates that some vegetation grew on the overbank sediment. At least some of the overlying coal was produced from *in situ* growth and accumulation of vegetation.

Argo Seam

Facies changes

The Argo seam changes facies regionally as well as locally within the mine. The nature of these changes aids reconstruction of the environment in which the Argo seam and first-generation lenses were deposited.

The seam is informally divided into two lithological units in the mine area. The 'Bottoms' are 3.3 to 4.0 m thick and consist of alternating beds of bright and moderately dull coal, the relative percentages of which vary little (Marshall &

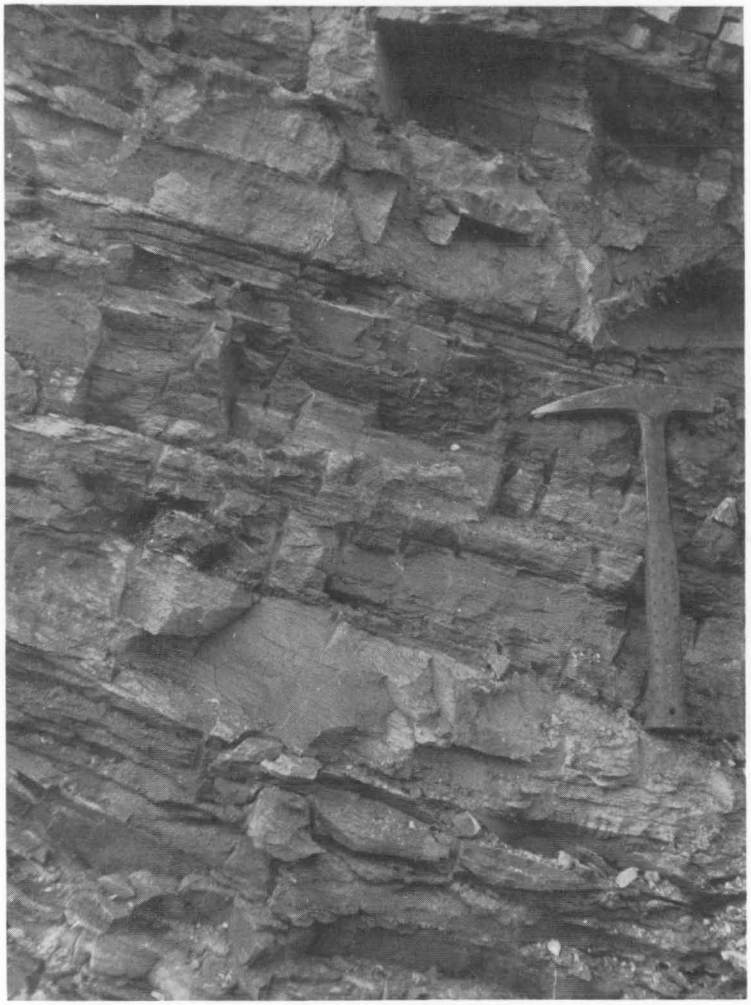

Fig. 29. Interbedded carbonaceous mudstone, siltstone, and fine-grained sandstone, second-generation lens at A6 (Fig. 5). Parallel lamination dominant; some ripple-drift laminated and cross-stratified sandstone beds.

Tompkins, 1966). In contrast, the 'Tops' consist of dull coal with minor bright bands and are quite variable in composition. The percentage of bright coal in the 'Tops' increases southward until south of C4+5 there is little lithological difference between the 'Bottoms' and 'Tops' (Marshall & Tompkins, 1966), and the division into two units becomes insignificant (Fig. 30). The pits studied for this Report were in the section along the outcrop belt where the bright coal content of the 'Tops' is sufficient to permit use of the full seam in the preparation of a coking coal product. However, the lithological difference between coking 'Bottoms' and non-coking 'Tops' persists northward from C4+5 at least to C4+37 (Fig. 30). The 'Main Lower' seam splits at C4+37 into the ?Orion and Gemini seams (Staines, 1972), which are separated by up to 24 m of grey shale. The Gemini seam splits into the Pollux and Castor seams north of C4+59 (Staines, 1972),

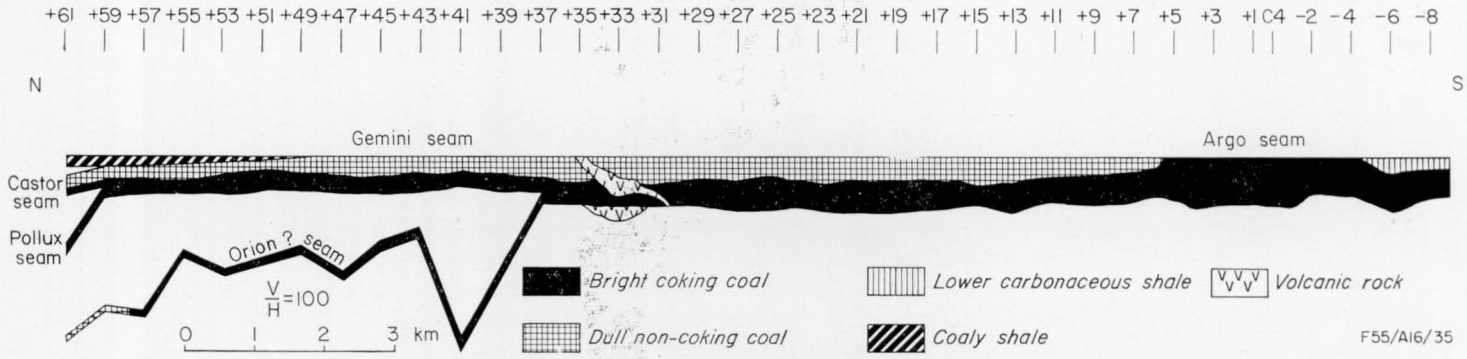

Fig. 30. Regional stratigraphy of the 'Main Lower' seam (adapted from Hansen, 1965, pl. 2).

Horizontal scale = 1:24 000. Scale $\frac{V}{H}$ = 50.

and the ?Orion, Pollux, and Castor seams deteriorate to carbonaceous shale north of the Central Railway (King, Goscombe, & Hansen, 1963).

Bright coal represents coalification of vegetation in a wetter environment than that which produces dull coal (CSIRO, 1971). Bright-coloured layers of peat record periods of flooding when anaerobic decay proceeds under stagnant water. Aerobic decay occurs during drier periods and produces dark-coloured peat (Deevey, 1958; Williams, 1971). Local and regional fluctuations of the water-table result in interbedding of bright-coloured and dark-coloured peat. CSIRO (1970a-j) has published lithological logs of the 'Main Lower' seam north of C4+12, which record these fluctuations in detail and confirm the regional picture of predominantly bright coal in the 'Bottoms' and predominantly dull coal in the 'Tops'.

During deposition of the 'Bottoms', conditions were generally wet throughout the mine area and north at least to C4+37. Moderately dull bands in the 'Bottoms' record short drier periods. During deposition of the 'Tops', however, environmental conditions were not uniform over that area; it was drier north of C4+5 where dominantly dark-coloured peat accumulated than south of that line where brighter-coloured peat formed. The water-table fell relative to the depositional surface north of C4+5 as the peat accumulated (CSIRO, 1971). South of C4+5 the relation between the depositional surface and the water-table changed very little during that time. This interpretation suggests that the rate of subsidence was relatively uniform across the area during deposition of the 'Bottoms', but that during deposition of the 'Tops' the rate of subsidence north of C4+5 decreased. South of C4+5 the rate of subsidence remained essentially unchanged, and wet conditions persisted during the deposition of the entire seam. First-generation depressions developed in the more rapidly subsiding wetter area. The percentage of bright coal in the 'Tops' continues to increase south of C4+5, and the upper part of the 'Tops' changes facies to the lower carbonaceous shale over the Deep Creek/Taurus split (Fig. 5, B1 to B7). These facies variations suggest that flooding was more common southward in the wetter area.

Environmental conditions were more stable south than north of C4+37 during deposition of the 'Bottoms'. Facies changes north of C4+37 during that time are recorded by the splitting of the ?Orion and Pollux seams from the Bottoms (Fig. 30). Too little is known about these splits to propose a mechanism for their development.

Fossil wood

Reddish brown fossil wood occurs in the coal at two localities in the mine. The wood varies from fragments a few centimetres long to logs 1.5 m long. Koppe (1972) describes the mineralization and degree of compaction which have affected this wood.

The long axes of 66 pieces of fossil wood exposed in the upper part of the coal near B8 (Figs 5, 19) in the Deep Creek/Taurus highwall show a strong preferred northwest orientation (Fig. 31a) (Koppe, 1972) which suggests that a stream flowed through the peat swamp at this locality. The stream flowed over an irregular peat floor, and clastic sediments in which bedforms could develop were not deposited in the channel. Without the influence of bedforms, the logs were probably oriented parallel to the current direction (Koppe, 1972). Palaeocurrents

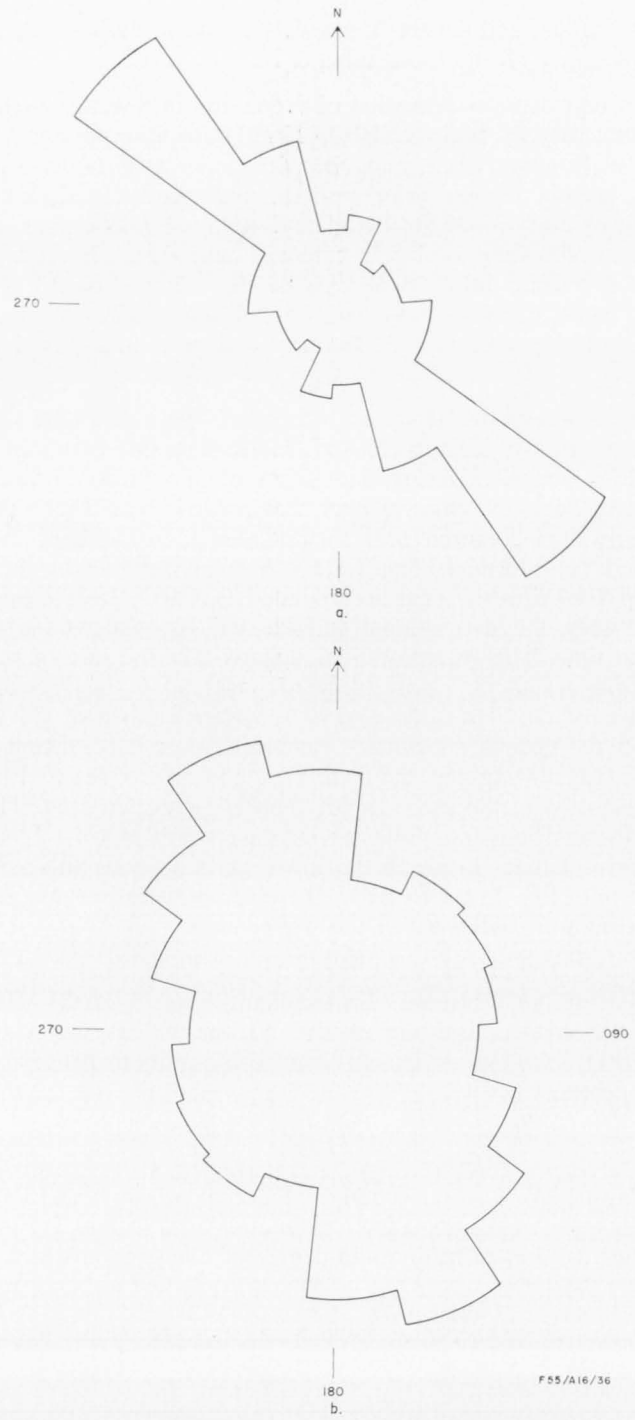

Fig. 31. Orientation of fossil wood long axes in the Argo seam (adapted from Koppe, 1972, fig. 2). (a) Deep Creek/Taurus highwall, B8 (Fig. 5), 66 measurements. (b) Stewarton pit, north of C5 (Fig. 6), 194 measurements.

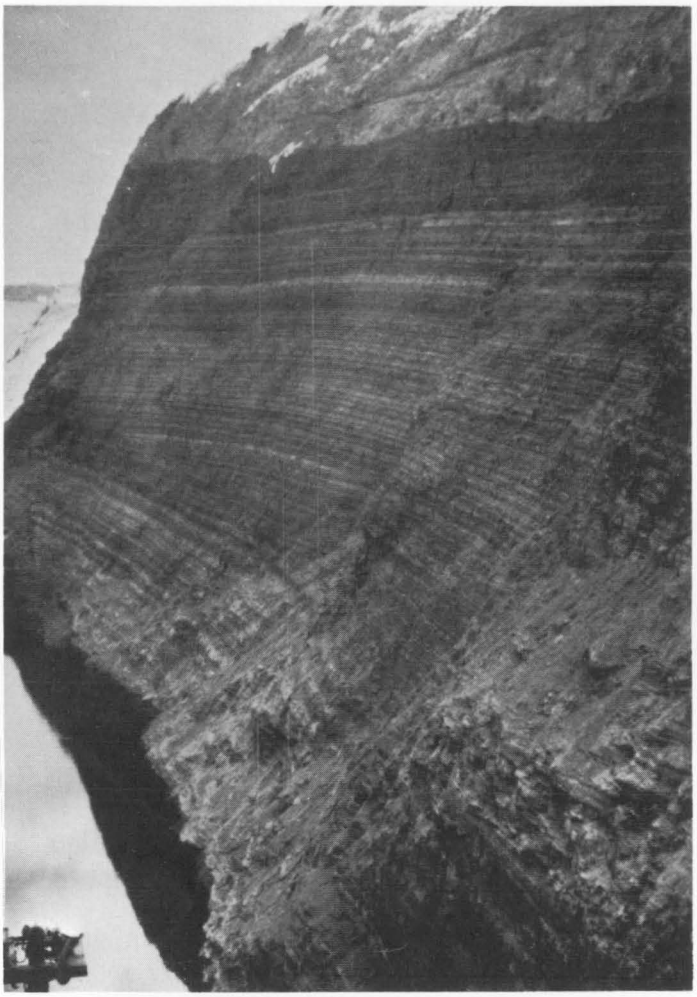

Fig. 32. Second-generation clastic rocks overlain by upper sandstone, north wall of Deep Creek/Taurus key-cut (Fig. 3). Second-generation beds are generally thin and laterally persistent, but some wedge out. Light-coloured upper sandstone lies on an erosional surface.

which deposited the lower sandstone flowed to the northwest; this evidence suggests that the stream in the peat swamp flowed northwestward rather than southwestward.

The long axes of 194 pieces of fossil wood exposed on the upper surface of the Argo seam in strip 1 from C4 – 9.5 to C4 – 10.5 in the Stewarton pit (Fig. 19) show a preferred orientation to the north-northwest (Fig. 31b) (Koppe, 1972). Fossil wood in the Stewarton pit is more widespread than in the Deep Creek/Taurus pit, but the orientations of fossil wood long axes in the coal are similar in both. The logs in the Stewarton pit were also probably deposited parallel to the current direction on an irregular peat surface. Currents confined to channels or flowing through ponded water oriented the wood as they moved north-northwestward across the peat in the northern end of the Stewarton pit.

Fig. 33. Even, parallel lamination in very fine-grained sandstone, second-generation lens at F3 (Fig. 6).

The presence of oriented fossil logs in the Argo seam is not evidence that it is a drift coal formed by plant debris transported from an area outside the coal basin. Rather, the restricted distribution of oriented logs in the coal suggests that local currents simply redistributed plant debris within an *in situ* peat deposit (Koppe, 1972). The presence of roots in strata below the coal, the considerable extent of the Argo seam, and the relative freedom of the coal from mineral matter also suggest an *in situ* swamp origin for the coal (Moore, 1940).

Lenses of Clastic Sedimentary Rocks

Sedimentary rocks in first, second, and third-generation lenses cannot be distinguished from each other on the basis of grainsize, sedimentary structures, or bedding characteristics. Abbreviations used in lithological logs are listed in Appendix 3.

Rock types

Laminated mudstone, laminated siltstone, and fine-grained ripple-drift laminated sandstone are the most common rock types in the lenses (Figs 29, 35). Individual beds are generally thin, laterally extensive, and have planar bounding surfaces (Fig. 32).

The mudstone is light grey to black and generally contains finely divided and whole plant remains. Laminated mudstone is commonly interbedded with siltstone laminae and very fine-grained cross-stratified sandstone. Non-laminated calcareous mudstone forms resistant massive beds. Subangular granules and pebbles of

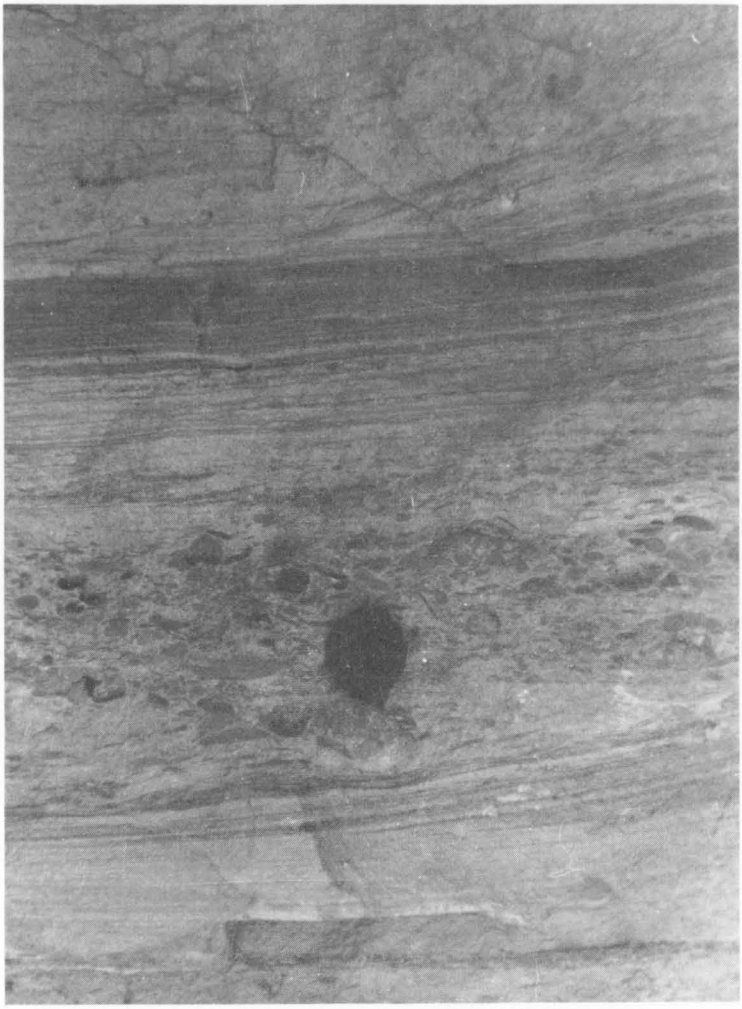

Fig. 34. Intraformational conglomerate interbedded with very fine to fine-grained, group cross-stratified carbonaceous sandstone, first-generation lens at B4 (Fig. 5).

laminated mudstone occur in non-laminated mudstone. The mud clasts may have formed during desiccation; when rewetted, some clasts disintegrated and the resulting sediment settled around other mud clasts to form a mud matrix. Small flammate structures along contacts between mudstone beds are associated with mudstone clasts and may also be products of desiccation. In one sample, several graded beds 0.5 cm thick consist of very fine-grained cross-stratified sandstone which grades upward into mudstone.

Light to dark grey carbonaceous siltstone is common in the lenses. Laminated siltstone contains mudstone interbeds and small lenses and laminae of very fine-grained sandstone. Massive siltstone is less common than laminated siltstone (Figs 35, 36).

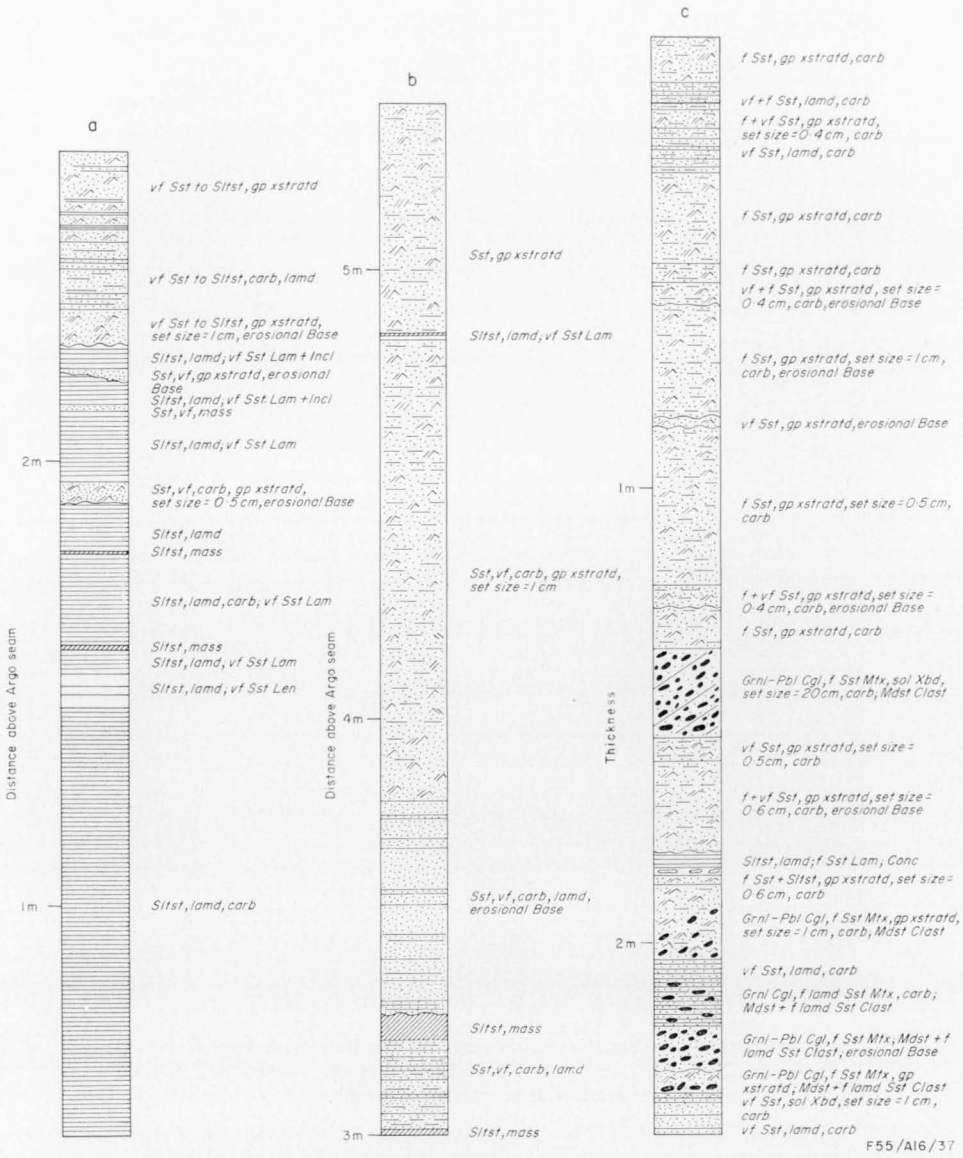

Fig. 35. Bedding characteristics of sedimentary rocks, U.D.C. mine.
Fig. 35a. Second-generation siltstone, Stewarton highwall, F3 (Fig. 6).
Fig. 35b. Second-generation sandstone, Stewarton highwall, F3 (Fig. 6).
Fig. 35c. First-generation sandstone, Deep Creek/Taurus split, B4 (Fig. 5). Abbreviations used in lithological logs are listed in Appendix 3.

Sandstone in the lenses is mainly light grey to buff, very fine to fine-grained, laminated, and ripple-drift laminated (Figs 33, 35, 36); the laminae are commonly delineated by carbonaceous material. Contemporaneous erosion and redeposition during periods of increased current flow is indicated in some places where group cross-stratified sandstone is interbedded with intraformational conglomerate (Figs 34, 35).

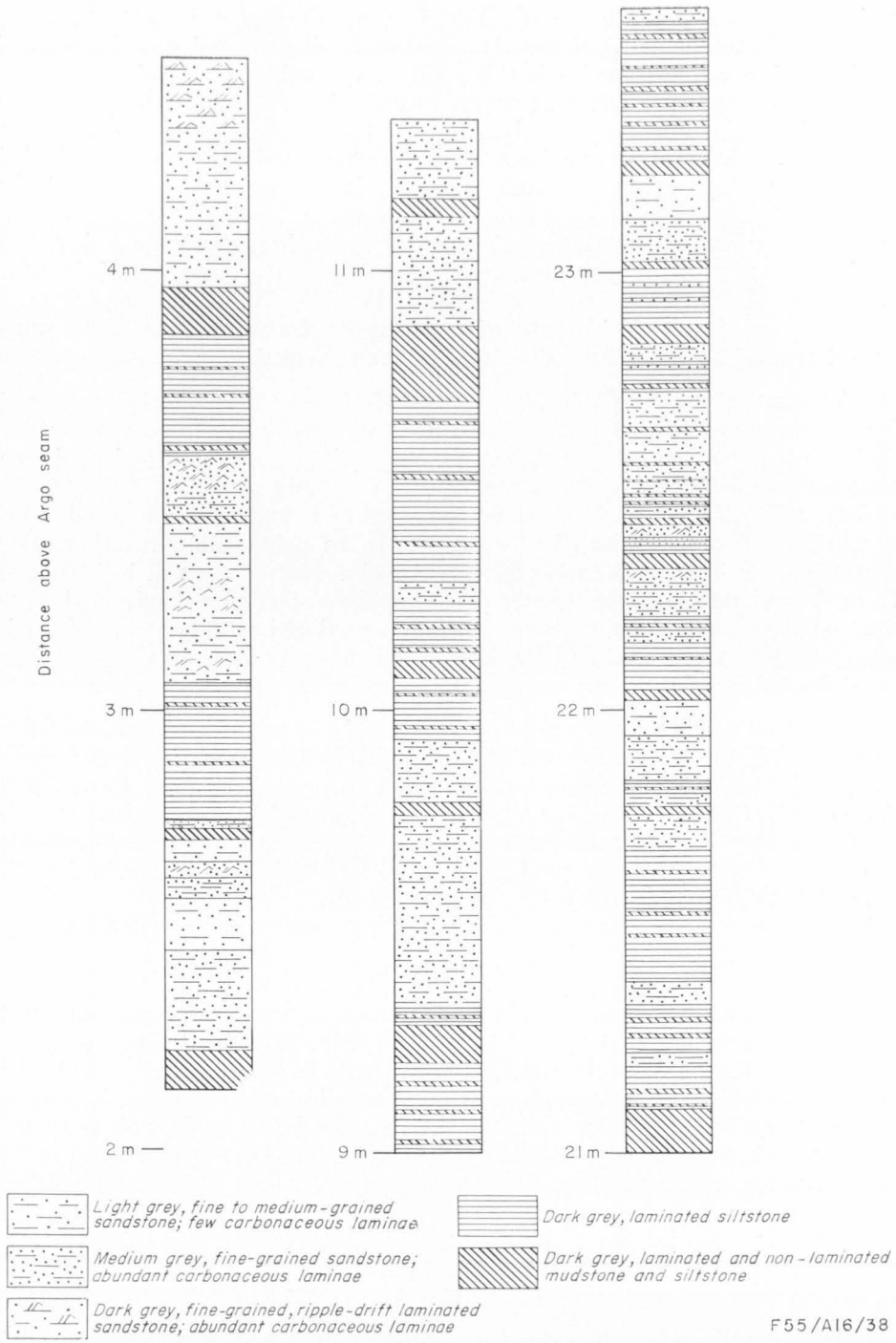

Fig. 36. Alternation of sandstone and siltstone in second-generation rocks, Deep Creek/Taurus key-cut.

The first-generation rocks which separate the Argo seam and lower carbonaceous shale from B8 to B9 (Fig. 5) along the highwall constitute a thin unit of brown mudstone which coarsens laterally to siltstone and very fine-grained sandstone between B8c and B9 (Fig. 37). The sandstone is dark grey, very carbonaceous, and laminated. It contains lenses and pods several centimetres long of very fine-grained light grey sandstone. Some lenses are localized thickenings in light grey ripple-drift laminated sandstone interbeds and may represent buried ripple crests. Pods and other lenses are dissociated from light grey interbeds; rolling of slightly consolidated sediment by currents, or slumping of soft sediment may have produced these structures. The dark grey sandstone facies with disturbed bedding occurs over the zone of oriented fossil logs in the Argo seam below the edge of the Deep Creek/Taurus split (Figs. 19, 37). The slumping or current activity responsible for bedding disturbance may be related to filling of the peat-floored channel in which the underlying logs were oriented.

The vertical sequence of bed types was studied in the Deep Creek/Taurus and Stewarton key-cuts (Fig. 3) to test for sedimentary cycles or rhythms in the lenses. Detailed descriptions of 7.5 m of interbedded sandstone, siltstone, and mudstone were made in the Deep Creek/Taurus key-cut (Fig. 36). A simple statistical test (Selley, 1970) shows that fine-grained laminated and ripple-drift laminated sandstone alternates with laminated siltstone; this is the only significant sedimentary rhythm present in these Deep Creek/Taurus rocks. The sequence of bed types in 12 m of similar rocks in the Stewarton key-cut shows the same simple sandstone-siltstone alternation. Variable energy conditions produced the alternation of sandstone and siltstone; its dominance in the rocks of the lenses indicates that they were not deposited in point bars.

The considerable lateral extent of individual beds, presence of persistent fine parallel lamination, and occurrence of graded beds indicate that sedimentary rocks of first, second, and third-generation lenses were deposited in lakes (Feth, 1964; Conybeare & Crook, 1968). The absence of medium and large-scale cross-stratification, presence of possible desiccation structures, and alternation of gentle currents with quiet-water conditions to produce sequences of interbedded fine-grained sandstone and siltstone also suggest lacustrine conditions.

Facies changes in the lenses

Clastic rocks in the lenses consist predominantly of mudstone throughout most of the mine area and north at least to C4+27 (Fig. 30), but the percentage of sandstone locally increases at several places in the mine. Sandy bodies occur in the first-generation Deep Creek/Taurus lens between B4 and B7 (Fig. 5), and in second-generation sedimentary rocks between F2 and F3 (Fig. 6) and above the lower carbonaceous shale between B5 and B9 (Fig. 5). They consist of up to 75 percent sandstone, contain cut-and-fill structures (Fig. 5, B6) and intraformational conglomerate (Fig. 5, B4), and are associated with smaller sandstone lenses. The sandy body between B4 and B7 lies at the southern end of the Deep Creek/Taurus lens. Its position near the mouths of possible flood channels tributary to this former depression suggests that it represents a small lacustrine delta.

The deposition of sandy bodies in a predominantly muddy sequence influenced the compactional evolution of sedimentary lenses into anticlines. Sandy areas of the lenses would stand higher than adjacent muddy areas after differential compaction

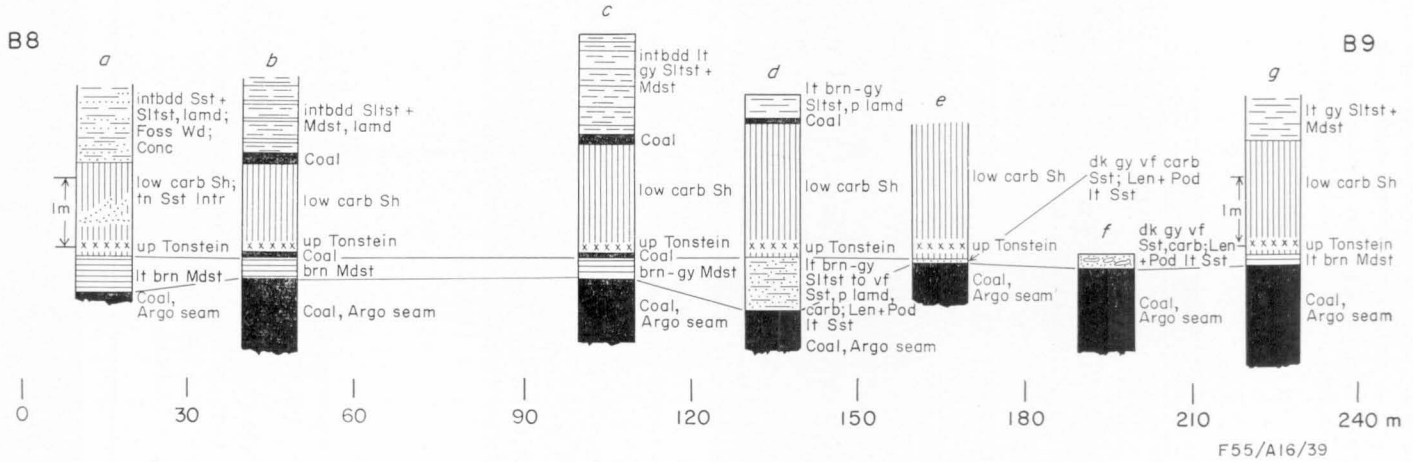

Fig. 37. Lithological logs of first and second-generation rocks, B8 to B9 (Fig. 5), Deep Creek/Taurus highwall.

and would become anticlines. The three sandy bodies observed in the mine occur at the cores of anticlines. However, the predominantly mudstone sequence in the lenses north of B1 (Fig. 5) is folded where no sandy bodies are present, and a syncline occurs in the sandy body at B8. The evolution of an anticline was controlled by differential compaction of the peat and sedimentary lens as a whole. The differential compaction of sand and mud within a lens made only a minor contribution.

Shape of the first-generation depressions

An isopach map of first-generation lenses which split the coal seam or the lower carbonaceous shale from the coal was plotted by computer (Fig. 37). It reveals several first-generation lenses which were not intersected by the highwall at the time of the survey. Two small roughly circular lenses centred on C4 – 7 and C4 – 10.5 were deposited in enclosed basins.

The Deep Creek/Taurus split (C4 – 1 to C4 – 6) and Stewarton split (C4 – 10.5 to C4 – 12.5) seen in cross-section in the highwall are shown to be elongate depressions with northwest-trending axes in plan view (Fig. 38). River channels would be open-ended along their axes in plan view; isopachs of channel-fills would not close at the ends of their axes. Palaeocurrents which deposited the lower sandstone and affected the Argo seam flowed towards the northwest. Deposition of the upper part of the coal was synchronous with deposition of first-generation sediments. Therefore, palaeocurrents which carried sediment to fill first-generation depressions must also have flowed toward the northwest. Both the Deep Creek/Taurus and Stewarton splits are closed on the southeastern, theoretically upstream ends of their axes. Discharge of sediment-laden water to the northwest through these depressions would therefore have been impossible. Sediments in these two splits were probably also deposited in enclosed basins. Subsurface data permit almost complete delineation of the Deep Creek/Taurus basin, but are insufficient to give a picture of the deepest part of the Stewarton basin.

The origin of the first-generation depression between C4 – 14 and C4 – 17.5 is less certain. The depression is open at the southeastern end of a northwest trending axis. The entire eastern part is undefined. This depression could be part of the channel of a northwest-flowing river or an enclosed basin.

Parts of several other first-generation lenses (C6+6.5 to C4+4, C4 – 9, C4 – 17 to C4 – 17.5) are shown in Figure 38. Those at C4 – 9 and C4 – 17 to C4 – 17.5 may represent enclosed basins, but too little is known about the shape of the other to indicate its origin.

The geometry of individual lenses indicates that rates of subsidence were variable within a basin. Two deep sub-basins are separated by a ridge (C4 – 3) within the Deep Creek/Taurus split basin (C4 – 1 to C4 – 6.5); subsidence in the northern section, where the lens is thin (C4 – 1 to C4 – 2), was slower and possibly later than elsewhere. In the Stewarton split (C4 – 10.5 to C4 – 12.5) subsidence was more rapid in the deeper western than in the eastern sub-basin.

Most first-generation depressions in the mine area are basins which formed as the result of differential compaction rather than river erosion; there is no evidence of widespread erosion of the coal below the splits. Clastic sediment which filled these basins must have been confined mostly to channels through the swamp

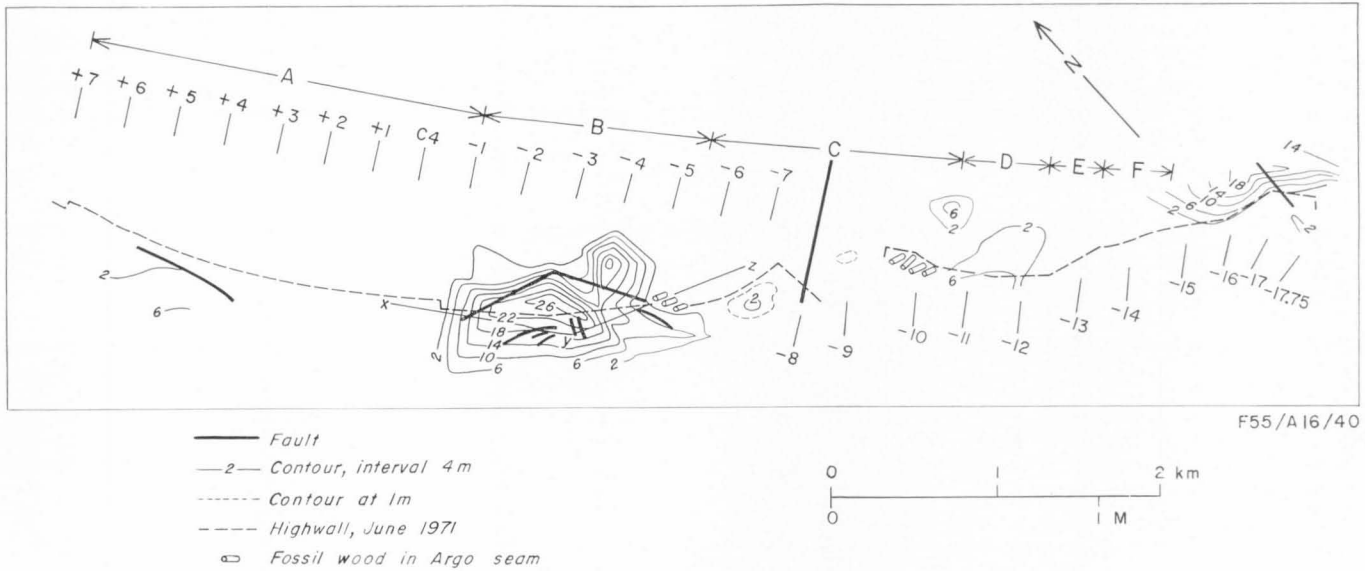

Fig. 38. Isopach map of first-generation lenses. Contour interval: 2 m.

before reaching them; sheet flooding over the swamp would have deposited clastic sediments between as well as in the basins. No widespread clastic beds separate the coal and lower carbonaceous shale between first-generation basins. However, no clear clastic channel-fill has been found tributary to a first-generation basin. The northwestward alignment of thin elongate lenses at C4 – 9 and C4 – 6.5 to C4 – 7.5 with the southern end of the Deep Creek/Taurus split at C4 – 6 indicates a possible tributary in that position. The small basins occupied by the two lenses may have acted as settling ponds along the course of a tributary to the large deep Deep Creek/Taurus basin (C4 – 1 to C4 – 6.5). Logs in the coal between C4 – 9.5 and C4 – 10.5 may have been oriented by flow along this tributary. Oriented logs in the coal between C4 – 5 and C4 – 5.5 probably record the position of a northwest-flowing flood channel tributary to that basin (Fig. 38). The Argo seam thickens and thins by as much as 6 m several times between C4 – 4 and C4 – 7 (Fig. 19), and the long axes of thick and thin areas trend toward the north-northwest. The northern group of oriented logs occurs where the seam thins rapidly. The data suggest that the local thickness changes in the Argo seam were produced by the erosion of flood channels tributary to the first-generation basin. At times of flood, water probably flowed between the basin lakes, which acted as sediment traps.

Lower carbonaceous shale

Facies and thickness variations. The lower carbonaceous shale was deposited in a marshy shallow lake south of C4 – 3 (Fig. 39) over peat and first-generation lenses. The black blocky shale contains plant remains, finely disseminated pyrite, and rare grey siltstone laminae. Thin interbeds of bright coal are common and reflect rapid burial in a wet environment before oxidation of the peat. North of C4 – 3 the land surface stood slightly higher during deposition of the lower carbonaceous shale; dark-coloured peat accumulated over the swamp and over lenses of clastic sediment under drier conditions in the north to form the upper part of the Argo seam 'Tops'.

Thickness variations of the lower carbonaceous shale reflect the topography which was developing on first-generation lenses during its deposition. The lower carbonaceous shale thins from 4.2 m on the flank of the Deep Creek/Taurus split at C4 – 5.5 to 0.6 m on the crest at C4 – 4 (Figs 38, 39). It also thins by 1 to 2 m over the crests of the small splits at C4 – 7 and C4 – 9 and is less than 1 m thick over most of the split between C4 – 14 and C4 – 17.5. This evidence suggests that the four lenses became slight mounds before or during deposition of the lower carbonaceous shale. Thickening of this unit between C4 – 5 and C4 – 8 indicates that a large depression flanked the three growing mounds at C4 – 1 to C4 – 6, C4 – 7, and C4 – 9. Depressions such as this represent an early stage in the development of second-generation basins on the flanks of first-generation mounds.

Some first-generation basins were still subsiding more rapidly than surrounding areas during deposition of the lower carbonaceous shale, which consequently thickens by almost 2 m both toward the centre of the small lens at C4 – 10.5 and toward the southeastern end of the large split at C4 – 14 to C4 – 17.5.

Thickness variations of the lower carbonaceous shale also reveal irregularities in the underlying peat surface that seem to be unrelated to first-generation lenses. High areas (Fig. 39, C4 – 10, C4 – 12) in the peat below thin areas in the lower

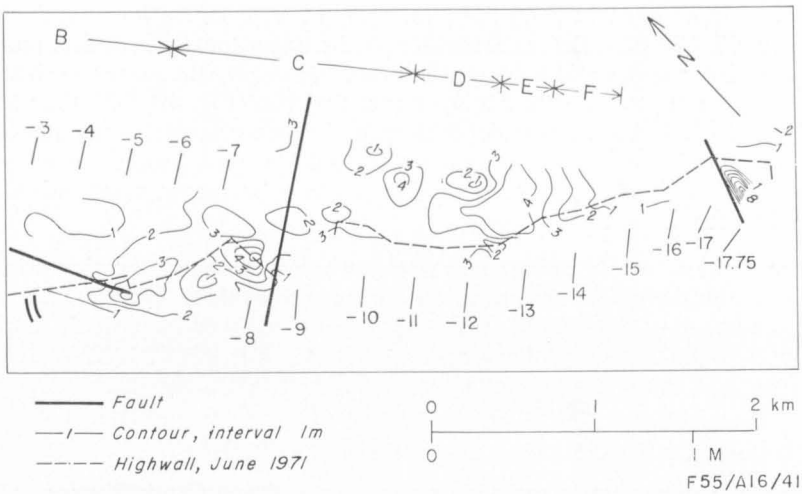

Fig. 39. Isopach map of lower carbonaceous shale. Contour interval: 1 m.

carbonaceous shale may reflect centres of relatively slow subsidence or of rapid peat accumulation.

Muddy peat accumulated over the northern end of the Deep Creek/Taurus split (C4 – 1 to C4 – 3) while the lower carbonaceous mud was deposited in the slightly lower, wetter area to the south. Thinning of the shaly coal toward the crest of the split confirms that this first-generation lens was becoming a mound during deposition of the muddy peat. Peat must have grown up the then gentle northern slope of the mound to form the shaly coal.

Upper tonstein. A thin persistent marker horizon informally called the upper tonstein was traced along the highwall from A1 to F3 (Figs 5, 6). It consists of 1 to 2 cm of calcareous sandy pinkish tan kaolinite and occurs within the lower carbonaceous shale or Argo seam or separates the two units. Appendix 2 contains a detailed petrographic description of the upper tonstein.

The lateral persistence of the thin kaolinite bed within carbonaceous rocks suggests that it represents a time horizon. Interpretations of the origin of tonsteins include: (1) oxidation of peat to produce a mineral residue from the ash content; (2) deposition in the peat-forming environment of detrital kaolinite derived from soil profiles in the source area; (3) alteration of beds of detrital sediment deposited in the acidic peat-forming environment to kaolinite; and (4) deposition and alteration of volcanic ash. W. Koppe (pers. comm.) feels that the considerable lateral persistence of this thin bed and the presence of fresh plagioclase, shard-like quartz fragments, and accessory apatite indicate that the upper tonstein is an altered pyroclastic unit.

Relative rates of subsidence during deposition of the lower carbonaceous shale can be determined by using the upper tonstein as a time horizon. Early during the deposition of the lower carbonaceous shale the relative rate of subsidence in the mine area was greatest over the Stewarton split (Fig. 6, D1 to D4). There the upper tonstein lies at its highest stratigraphic position, in the middle of the lower

carbonaceous shale (Fig. 40, D2). On the flanks of the split (Fig. 6, C3 to D1, D4 to E2) the upper tonstein lies within but near the base of the lower carbonaceous shale (Fig. 40, C3, E2). Before deposition of the upper tonstein this first-generation basin subsided more rapidly than its flanks. However, the lower carbonaceous shale above the upper tonstein is thinner over the split (Fig. 40, D2) than adjacent to it (Fig. 40, C3, E2). After deposition of the upper tonstein, the rate of subsidence in the basin decreased relative to that in surrounding areas, possibly because the lens of first-generation sediments was becoming a mound owing to differential compaction.

The relative rate of subsidence was much less south of the Stewarton split throughout the deposition of the lower carbonaceous shale (Fig. 6, E3 to F3). Peat accumulated there until the upper tonstein was deposited, and little carbonaceous shale was laid down over it (Fig. 40, E3, F2, F3). This area was a relative high in the southern wetter zone; its slight elevation reflected growth of an anticline below the peat (p. 21) or rising of the first-generation lens between C4 – 14 and C4 – 17.5 (p. 48, Fig. 38; Fig. 6, south of F3).

The rate of peat accumulation north of the Deep Creek/Taurus split was uniform after deposition of the upper tonstein (Fig. 41, A1 to A5). The presence of the upper tonstein in both the lower carbonaceous shale on the southern flank and the shaly coal on the northern flank of the split proves that these units are facies equivalents.

A brown kaolinite tonstein called the pellet claystone (Appendix 2) is a persistent marker 1 cm thick in the lower part of the Argo seam throughout the mine area. Like the upper tonstein, the pellet claystone probably represents a time horizon. The peat which accumulated during the time between deposition of the pellet claystone and upper tonstein is thinner between A2 and A5 than at A1 (Figs 5, 41). Growth of the anticline below the seam between A3 and A5 (p. 23) during peat accumulation may have caused the thinning.

Upper Sandstone

Fine to medium-grained cross-stratified sandstone similar to the lower sandstone overlies lacustrine beds in the lenses of clastic sedimentary rocks. This unit is informally called the upper sandstone because of its position at the top of the highwall. Utah Development Company maps show that it occurs throughout the mine area on the eastern down-dip edge of the projected open cut (Hansen, 1965). The upper sandstone is exposed in the Deep Creek/Taurus and Stewarton key-cuts (Fig. 3) and in the highwall from A1 to A5 (Fig. 5) and at C4 (Fig. 6). It is at least 14 m thick.

The upper sandstone lies on an erosional surface which was cut into the underlying lacustrine basin-fill sediments (Fig. 32). The lower part of the unit is a conglomerate of siltstone and mudstone granules and pebbles in a medium to coarse-grained sandstone matrix. The light grey to buff sandstone is characterized by large-scale trough cross-stratification and ripple-drift lamination, and higher in the unit it is interbedded with shale (Hansen, 1965). Prominent cut-and-fill structures occur in the upper sandstone near A3 (Fig. 5) and at C4 (Fig. 6). These characteristics and its similarity to the lower sandstone indicate that the upper sandstone is also a point-bar deposit: a river channel migrated back into

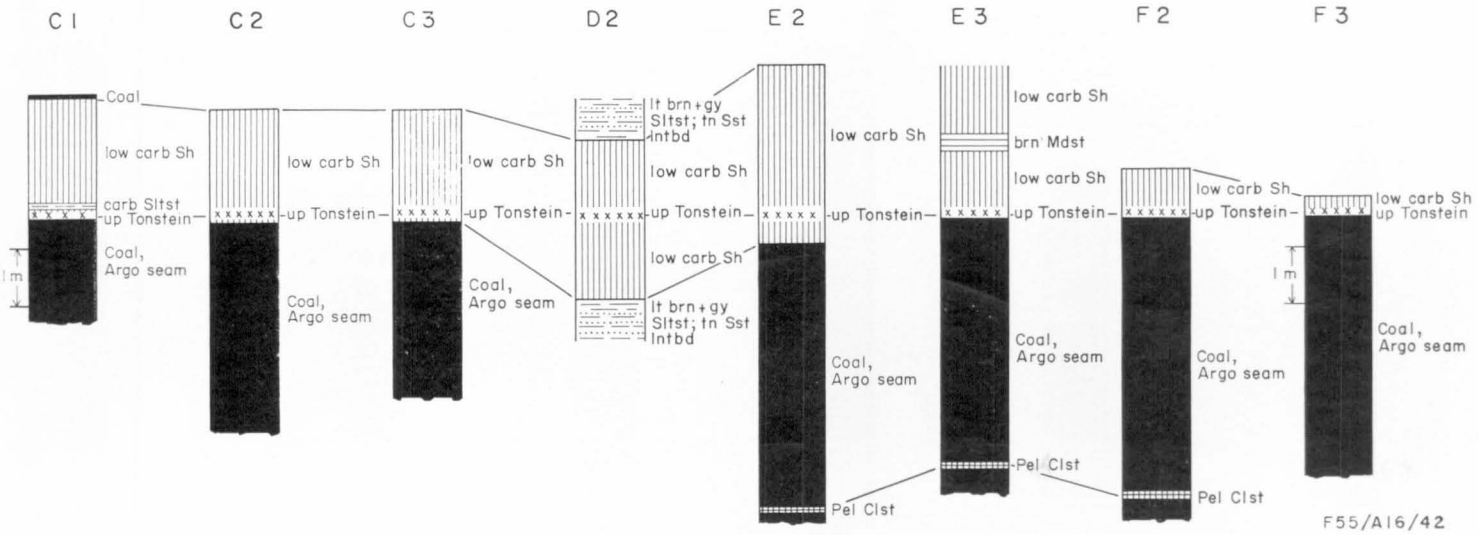

Fig. 40. Lithological logs of Argo seam and lower carbonaceous shale, Deep Creek/Taurus and Stewarton highwalls, C1 to F3 (Figs 5, 6).

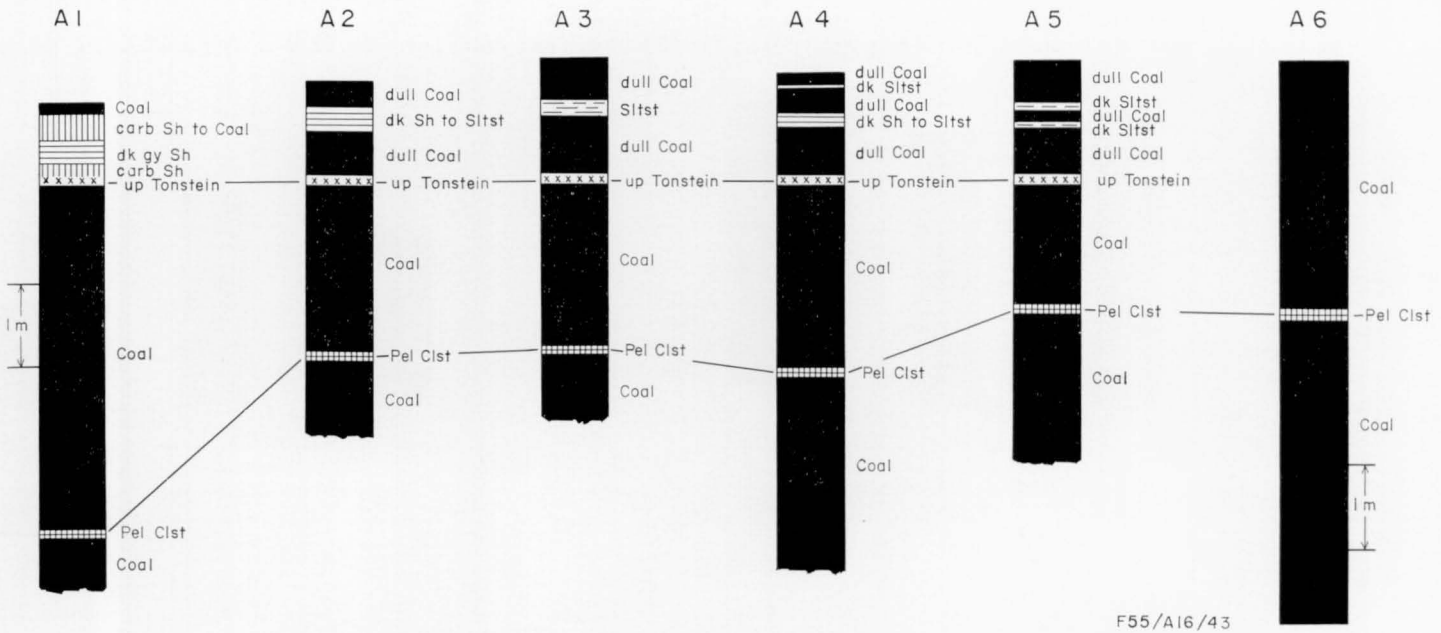

Fig. 41. Lithological logs of Argo seam, Deep Creek/Taurus highwall, A1 to A6 (Fig. 5).

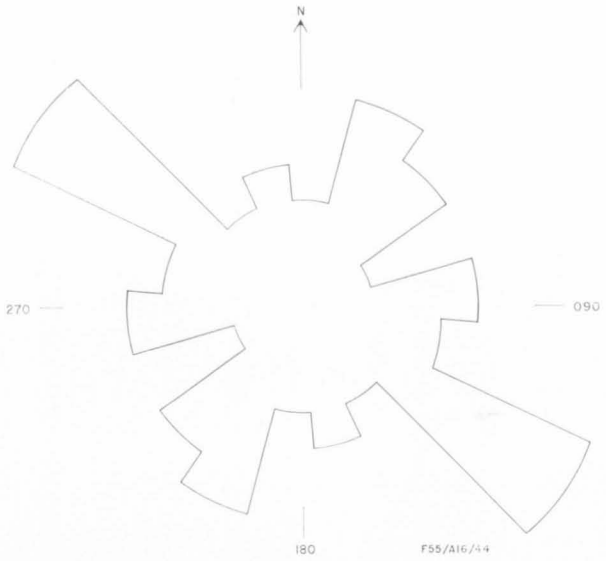

Fig. 42. Orientation of fossil wood long axes in upper sandstone, Deep Creek/Taurus and Stewarton key-cuts; 41 measurements.

the mine area, slightly eroded the lacustrine sediments, and laid down channel and overbank sediments (Fig. 43).

Large fossil logs are concentrated in the carbonaceous basal part of the upper sandstone throughout the mine area (Hansen, 1965). The long axes of the fossil wood have a preferred northwest orientation with secondary trends at oblique and right angles (Fig. 42). Palaeocurrent directions in the lower sandstone and Argo seam were to the northwest. The data suggest that fossil logs in the upper sandstone were oriented by currents which also flowed to the northwest; the orientation of logs to the northeast and east may have been caused by the influence of bedforms. However, as in the lower sandstone, the predominant orientation of fossil wood may reflect the influence of bedforms as well as the current direction itself (p. 31). Intense weathering of the upper sandstone prevented measurement of the orientation of cross-strata.

Interpretation of the Vertical Profile

The section of the Rangal Coal Measures exposed in the mine was deposited in a fluvial environment (Fig. 43). The migration of a channel from the mine area led to the deposition of muddy overbank sediment above slightly older point-bar sediment, and a peat swamp grew on the flood plain. When sediment-laden floodwater flowing through ephemeral channels reached depressions in the swamp, clastic sedimentation began in the shallow basins. Three generations of flood-plain lakes filled with sediment to form a single genetic basin-fill unit. A river channel migrated into the mine area, slightly eroded the lacustrine sediments, and deposited the upper sandstone in point bars.

Palaeocurrents which deposited the lower sandstone flowed to the northwest. The orientation of fossil wood long axes in the Argo seam and upper sandstone

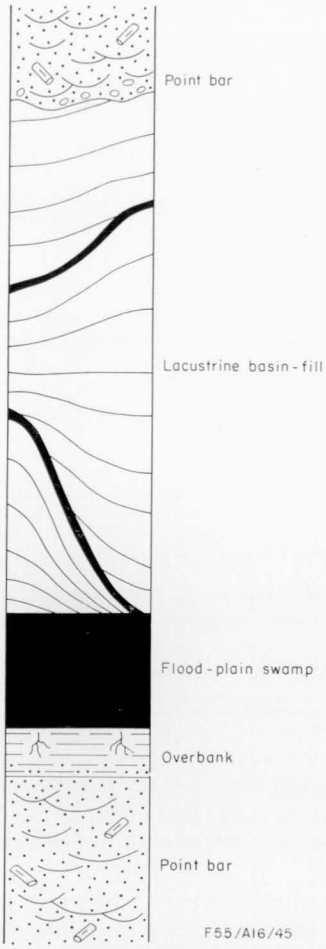

Fig. 43. Diagrammatic vertical profile, Rangal Coal Measures, U.D.C. mine.

suggest that palaeocurrents flowed to the northwest. This apparent coincidence of palaeocurrent direction through the section indicates that changes in the vertical profile were caused by the lateral migration of a single river system.

PALAEOGEOGRAPHIC EVOLUTION OF THE MINE AREA

The palaeogeographic evolution of the mine area during deposition of the Rangal Coal Measures was controlled by the lateral migration of river channels and by differential compaction of organic and inorganic sediment in space and time. The local folds at Blackwater were produced by the compaction of clastic sediments deposited in small lakes on a river flood plain.

During deposition of the lower sandstone a meandering river flowed to the northwest and deposited point bar sands (Fig. 44-1). As the river channel

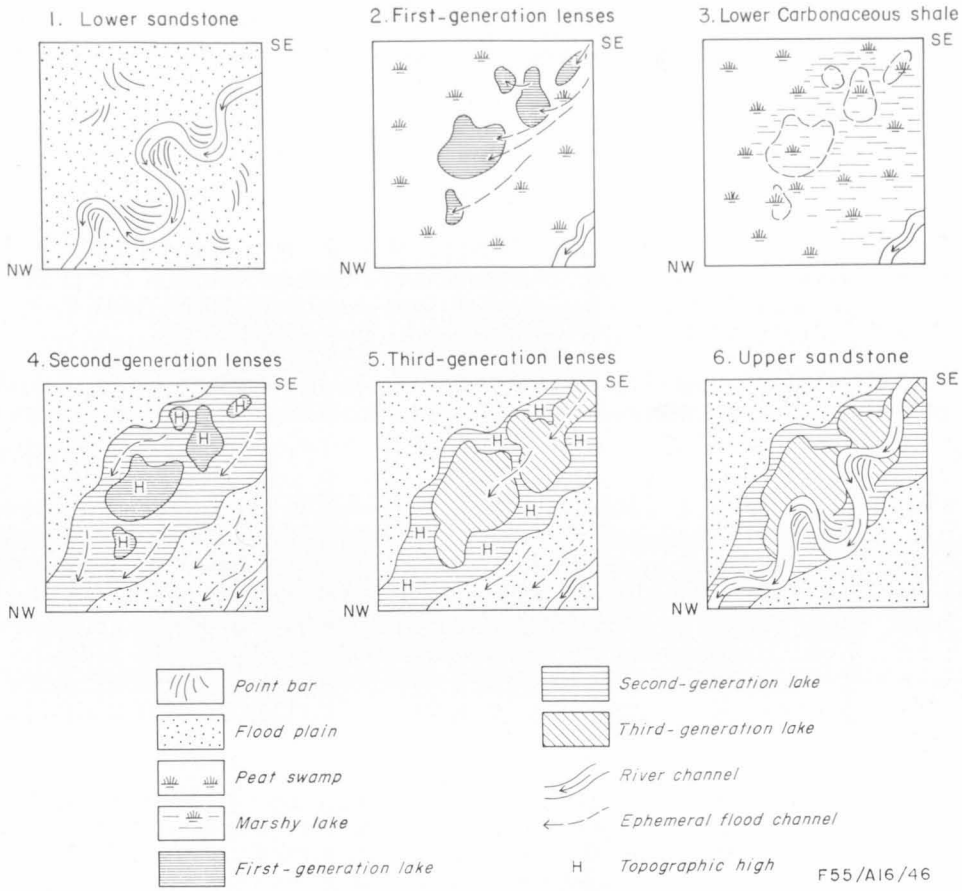

Fig. 44. Palaeogeographic evolution of the U.D.C. mine area during deposition of the Rangal Coal Measures.

migrated from the mine area, abandoned point bars on the flood plain were partly buried by the overbank deposits of the grey mudstone. A peat swamp developed on the flood plain over slightly irregular topography. As the weight of the accumulating peat increased, the underlying sandy point-bar and muddy overbank sediments began to be compacted differentially, and anticlines developed in sandy areas. The peat was compacted uniformly under its own weight, and depressions formed in the swamp surface over depressions in the buried flood-plain topography or over areas between growing anticlines. Differential accumulation and compaction of peat caused by botanical or groundwater conditions may also have contributed to the development of depressions. Plant material accumulated in the depressions until sediment-laden floodwater reached them through ephemeral channels, which probably flowed northwestward through the swamp (Fig. 44-2). Horizontal beds of sediment were deposited in shallow lakes in the depressions, and the sediment load caused more rapid compaction of the peat below these basins. The rate of basin subsidence eventually decreased as the peat below the basins became more compacted, and the first-generation lakes shoaled or filled with sediment. The greater compactional potential of peat adjacent to the first-

generation basins caused the rate of subsidence to be more rapid there than below the basins. The slowly subsiding, relatively incompressible lenses of clastic sediment which filled the lakes began to evolve into mounds in the swamp. Strata in the lenses were folded as the mounds developed.

A shallow marshy lake formed in the lower wetter part of the swampy flood plain in the southern part of the mine area (Fig. 44-3). Floodwater spread across the swamp in a sheet as the compactional growth of mounds in the positions of former basins disrupted the system of ephemeral channels and small lakes. Some first-generation basins in the floor of the marshy lake were still subsiding, and thicker deposits of carbonaceous mud accumulated in them than over rising first-generation lenses. During the late stage of deposition of the lower carbonaceous shale these basins filled and also began to develop into mounds.

A second-generation lake basin developed in the more rapidly subsiding area which surrounded the first-generation mounds or islands (Fig. 44-4). Clastic sediment carried by flood channels was deposited in the lake. The differential compaction of point-bar and overbank sediments below the peat was producing anticlinal ridges in the floor of the second-generation lake; the ridges divided the lake into sub-basins. The anticlines and first-generation mounds were slightly eroded before they were buried by sediment. The second-generation basin filled when the rate of compaction of peat below it decreased. Relatively rapid compaction of peat below first-generation lenses caused the second-generation lens of lacustrine sediment to begin developing into a group of mounds, and second-generation sediments were folded. Initial stages of this reversal of topography disrupted the circulation of the second-generation lake system. A shallow marshy lake in which the upper carbonaceous shale was deposited flooded the mine area.

A third generation of lake basins developed between second-generation mounds as their relief continued to increase (Fig. 44-5). These small basins roughly coincided with first-generation basins. Ephemeral flood channels carried sediment into the lakes. Third-generation clastic lenses were not folded into anticlines by a reversal of topography.

A meandering river channel migrated into the mine area (Fig. 32-6), slightly eroded the lacustrine sediments, and deposited the point-bar and overbank sediments of the upper sandstone.

ECONOMIC SIGNIFICANCE OF THE FOLDS

Decreased coal quality and instability of mine walls are related in places to compactional folds of the type studied at Blackwater. Britten (1972) points out that compactional folding and faulting of the Singleton Coal Measures have produced weakened zones which will cause locally poor roof conditions as underground mining proceeds. Prediction of the occurrence and geometry of compactional folds is therefore important in planning mine design and development in a coalfield. Britten (1972) feels that even though some compactional folds can be located by bore data, their effects on mining are difficult to assess because of the localized distribution and variable geometry of the structures. Methods for predicting the locations of compactional folds in some stratigraphic situations have been developed in this Report.

Coal Quality

A zone of high-ash durain with poor washability characteristics was unexpectedly encountered in the Argo seam below the northern end of the Deep Creek/Taurus split (Figs 38, C4 – 1 to C4 – 3.5; 5, B1 to B3) (Williams, 1971). During initial stages of its development, the split was a slight depression in which coal-forming vegetation was deposited. Water carrying fine clastic sediment from higher surrounding areas in the swamp also collected in the basin, producing dirtier peat in the depression (Williams, 1971). Deposition of the high-ash coal ceased when floodwater delivered large volumes of clastic sediment to the basin (p. 55).

High-ash coal may occur in a seam wherever a local basin existed during peat formation. If the volume of clastic sediment supplied to the basin and the rate of subsidence within it varied as vegetation was deposited, high-ash coal would have formed in a sub-basin rather than continuously across the basin. The irregular topography of the Deep Creek/Taurus split lens indicates that the rate of subsidence varied across the basin (p. 48). Therefore, the zone of high-ash coal below the northern end of the split may occupy only a small area of the original basin. Prediction of the locations of first-generation basins can only indicate possible areas of high-ash coal. Precise delineation of these zones must be based upon examination of coal samples.

Compactional faults and fossil wood associated with seam splits of the Blackwater type may also adversely affect coal washability and processing. Loading of the Argo seam peat by clastic sediment in the Deep Creek/Taurus lens caused compactional adjustments during the evolution of the lens to a mound (p. 23). Faults which record these movements thrust wedges of mudstone, sandstone, and carbonaceous shale into the Argo seam below and at the edges of the split (Figs 9, 10, 23, 25, 38). Coal from faulted areas which contain these wedges may require special processing. Local zones of oriented fossil wood in the Argo seam probably record the positions of flood channels tributary to the Deep Creek/Taurus split basin (p. 39). Occurrences of mineralized wood in the seam are therefore spatially related to splits. Local thickening and thinning of the seam caused by the erosion of flood channels may be associated with oriented fossil wood (p. 48).

The contribution of an economic seam to a coking coal product may thus be very limited from areas below and alongside a split by inorganic sediment introduced during peat deposition and compactional faulting, and by local erosion during and after peat formation.

Instability of Mine Walls

The Utah Development Company Blackwater open-cut mine runs parallel to the strike of the Argo seam, and each successive strip is located down-dip from previous cuts; but bedding in the overburden does not always dip away from the highwall because of the presence of discordant folds above the Argo seam. The mine highwall has been unstable in areas where overburden beds dip toward it (E. N. Milligan, pers. comm.).

Drilling data show that the lower carbonaceous shale splits from and rejoins the Argo seam and forms domes. Bedding in the lenses between this marker and the Argo seam is predicted to be concordant with the domed marker horizon.

Designing a pit to minimize highwall instability is difficult when coal must be removed from areas below domal structures. Regardless of the orientation of the highwall relative to a dome, it must in some strips intersect beds which dip toward it. Beds in the Deep Creek/Taurus lens which dipped toward the highwall have now been mostly removed, and future strips across this dome will cut beds which dip away from the highwall (Fig. 38, B).

Once the location and geometry of a dome are known, areas of possible highwall instability can be predicted. Some folds above and discordant with the Argo seam and lower carbonaceous shale at Blackwater (Figs 5, A1 to A6, B5 to B9; 6, F1 to F3) were not discovered during drilling because no marker bed, such as a carbonaceous layer, occurs in or overlies them. A technique other than drilling must be developed to predict the location and geometry of such folds and areas of possible highwall instability caused by them.

Prediction of the Location and Geometry of the Folds

Folds of the Blackwater type may occur in coal measures wherever the surface below a thick coal seam shows depositional or compactional relief. The morphology of the surface below the peat controlled the development of folds above the Argo seam at Blackwater. The morphology of that surface was determined by (a) the topography of the area when deposition of point-bar sand (lower sandstone) ceased; (b) the distribution and variable thickness of overbank mud (grey mudstone) which partly buried the sand; and (c) the differential compaction of the sediments. The vertical subsidence caused by peat compaction, the depth of resulting basins, and the thickness of split lenses increase with the thickness of a peat seam. A thick accumulation of peat is necessary to produce structures of the magnitude of folds at Blackwater.

Discordant folds may be predicted above a coal seam with the help of a structure contour map of the base of the seam and of lithofacies and isopach maps of rocks below the seam. These data are especially useful where a single seam is to be mined and marker beds do not occur above it. Because exploratory drill holes penetrate a prospective seam, a structure contour map of its base can be drawn as mine development is planned. Basins which formed in the peat swamp would have been located between local ridges shown on the structure contour map (pp. 11, 13). These local ridges were probably produced by differential compaction of sandy and muddy sediments below the seam. Therefore, knowledge of the distribution and shape of relatively incompressible sand bodies below the seam may assist in predicting the positions of local ridges and associated basins. Drill holes at Blackwater penetrated an average of 1 m below the Argo seam and indicate where the lower sandstone directly underlies the seam; many holes, however, were not deep enough to strike the contact of the lower sandstone and grey mudstone. Consequently, thickness variations of the grey mudstone which affect differential compaction of the sedimentary column could be delineated for only small areas of the mine. Drilling deeper below the Argo seam would have permitted more complete reconstruction of the lithofacies pattern which determined the locations of basins in the swamp; but it would not be economically justified unless other data were inadequate to predict the locations of folded basin-fill strata.

The development of folds in sediment which fills basins in a peat swamp depends upon differential compaction of the basin-fill sediments and underlying

peat. Therefore, if such a basin fills with vegetable material rather than clastic sediment, this organic sediment and the underlying peat seam will not be compacted differentially, and discordant folds related to that basin will not overlie the resulting coal seam. An anticline of C4+4 is shown by structure contours on the base of the Argo seam (Fig. 7), and a first-generation basin would thus be predicted to lie north of that line. Thickening of the vertical section of the Argo seam between the pellet claystone and upper tonstein northward from A2 to A1 (Fig. 41) indicates that such a basin did exist (p. 50) and that it filled with organic matter while other first-generation basins filled with clastic sediment. The folds in clastic beds above the Argo seam north of A2 are not related to the compactional history of this organic basin-fill; they were produced by differential compaction of a second-generation clastic basin-fill unit (pp. 19-21). The geometry of folds above the seam in this area could not be predicted from the knowledge of the location and shape of the first-generation basin in the peat swamp.

Prediction of the structure of clastic sedimentary rocks in coal measures is facilitated when marker beds are common in the sequence, or several seams are to be mined in the same area. Exploratory drilling will penetrate the base of the lowest economic seam and all overlying marker beds. Structure contours on all carbonaceous and other marker beds and isopach maps of sediment bodies between them can then be drawn. When a marker bed directly related to the top of a coal seam is folded above the seam, it locates first-generation basins which filled with clastic sediment in a peat swamp. Once the first-generation palaeogeography is known, the location and geometry of folds in younger sediments may be predicted according to the general model presented here: anticlines develop over former depressions, and synclines develop over areas which were high during clastic deposition. Structure-contour maps of the base of the Argo seam and lower carbonaceous shale are sufficient information to reconstruct the geometry of folds above them at Blackwater; knowledge of the structure of the upper carbonaceous shale permits confirmation of the existence of the predicted folds.

In coalfields where a marker bed delineates first-generation clastic basin-fill sediments in a coal seam, the location of possible areas of high-ash coal and of folds which may cause highwall instability can be predicted from structure-contour maps of the coal seam and marker bed. In coalfields where no marker beds overlie the seam to be mined, structure-contour maps of the seam and lithofacies and isopach maps of sedimentary rocks below the seam may identify locations of first-generation basins and therefore possible areas of high-ash coal. However, the clastic or organic nature of the basin-fill sediments cannot be predicted in the absence of marker beds above the seam; consequently, the pattern of folds and of possible highwall instability cannot be completely predicted.

REFERENCES

ALLEN, J. R. L., 1965a—A review of the origin and characteristics of recent alluvial sediments. *Sedimentology*, 5, 89-191.

ALLEN, J. R. L., 1965b—Fining-upwards cycles in alluvial successions. *Geol. J.*, 4, 229-46.

BRITTEN, R. A., 1972—A review of the stratigraphy of the Singleton Coal Measures and its significance to coal geology and mining in the Hunter Valley region of New South Wales. *Aust. Inst. Min. Metall. Conf., Newcastle,* 1972, 11-22.

BRUNT, D. A., 1969—Sedimentology and stratigraphy of the Caloundra area, south-east Queensland. *Hon. Thesis, Dep. Geol., Univ. Qld.* (unpubl.).

CONYBEARE, C. E. B., & CROOK, K. A. W., 1968—Manual of sedimentary structures. *Bur. Miner. Resour. Aust. Bull.* 102.

CSIRO, 1970a—Report on Main Lower seam from Blackwater Borehole N.S. 100, Blackwater district, central Queensland. *CSIRO Div. Miner. Chem. Location Rep.* 372.

CSIRO, 1970b—Report on Main Lower seam from Blackwater Borehole N.S. 102R, Blackwater district, central Queensland. *Ibid.*, 373.

CSIRO, 1970c—Report on Main Lower seam from Blackwater Borehole N.S. 97, Blackwater district, central Queensland. *Ibid.*, 374.

CSIRO, 1970d—Report on Main Lower seam from Blackwater Borehole N.S. 96, Blackwater district, central Queensland. *Ibid.*, 376.

CSIRO, 1970e—Report on Main Lower seam from Blackwater Borehole N.S. 86, Blackwater district, central Queensland. *Ibid.*, 377.

CSIRO, 1970f—Report on Main Lower seam from Blackwater Borehole N.S. 106R, Blackwater district, central Queensland. *Ibid.*, 378.

CSIRO, 1970g—Report on Main Lower seam from Blackwater Borehole N.S. 95, Blackwater district, central Queensland. *Ibid.*, 379.

CSIRO, 1970h—Report on Main Lower seam from Blackwater Borehole N.S. 88, Blackwater district, central Queensland. *Ibid.*, 380.

CSIRO, 1970i—Report on Main Lower seam from Blackwater Borehole N.S. 94, Blackwater district, central Queensland. *Ibid.*, 381.

CSIRO, 1970j—Report on Main Lower seam from Blackwater Borehole N.S. 93, Blackwater district, central Queensland. *Ibid.*, 382.

CSIRO, 1971—Petrography as guide to origin of some Permian coals. *Coal Res. in CSIRO,* 44 (July), 2-6.

DAVIS, A. (Ed.), 1971—Proceedings of the Second Bowen Basin Symposium. *Geol. Surv. Qld Rep.* 62.

DEEVEY, E. S., Jr, 1958—Bogs. *Sci. Amer.*, 199(4) 114-22.

DICKINS, J. M., & MALONE, E. J., 1973—Geology of the Bowen Basin, Queensland. *Bur. Miner. Resour. Aust. Bull.* 130.

FETH, J. H., 1964—Review and annotated bibliography of ancient lake deposits (Precambrian to Pleistocene) in the Western States. *U.S. geol. Surv. Bull.* 1080.

HANSEN, W. A., 1965—Report on geology of the C4+7000 test pit area. Appendix I *in* Thompson, B. R.—Report on test pit investigations C4+7000 area, Blackwater Coal Field. *Utah Devel. Co. Rep.* 136 (unpubl.).

JENSEN, A. R., 1968—Upper Permian and Lower Triassic sedimentation in part of the Bowen Basin, Queensland. *Bur. Miner. Resour. Aust. Rec.* 1968/55 (unpubl.).

JENSEN, A. R., 1971— Regional aspects of the Upper Permian regression in the northern part of the Bowen Basin. *Geol. Surv. Qld Rep.* 62, 7-20.

JENSEN, A. R., in press—Permo-Triassic stratigraphy and sedimentation in the Bowen Basin. *Bur. Miner. Resour. Aust. Bull.* 154.

KING, D., GOSCOMBE, P. W., & HANSEN, W. A., 1963—Report on Stage II investigations, Blackwater district, central Queensland. *Utah Devel. Co. Rep.* 115 (unpubl.).

KIRKEGAARD, A. G., 1970—Duaringa, Qld—1:250 000 Geological Series. *Bur. Miner. Resour. Aust. explan. Notes* SF/55-16.

KOPPE, W. H., 1972—Fossil wood orientation within the 'Main Lower' seam, Utah open cut mine, Blackwater. *Qld Govt Min. J.*, 73, 370-72.

MALONE, E. J., OLGERS, F., & KIRKEGAARD, A. G., 1969—The geology of the Duaringa and Saint Lawrence 1:250 000 Sheet areas, Queensland. *Bur. Miner. Resour. Aust. Rep.* 121.

MARSHALL, C. E., & TOMPKINS, D. K., 1966—Blackwater Coalfield: Quality, preparation, and carbonisation characteristics of the Main Lower seam of the Blackwater mine area. *Coal Res. Group, Dep. Geol. Geophys., Univ. Sydney* (unpubl.).

MOORE, E. S., 1940—COAL. *N.Y., Wiley.*

PATEN, R. J., 1971—Permian geology, central-western Bowen Basin. *In* Playford, G. (Ed.)—Geological excursions handbook. *43rd ANZAAS Cong., Brisbane,* 21-43.

PELLETIER, B. R., 1958—Pocono paleocurrents in Pennsylvania and Maryland. *Bull. geol. Soc. Amer.,* 69, 1033-64.

POTTER, P. E., & PETTIJOHN, F. J., 1963—PALEOCURRENTS AND BASIN ANALYSIS. *Berlin-Heidelberg, Springer.*

RAISTRICK, A., & MARSHALL, C. E., 1939—THE NATURE AND ORIGIN OF COAL AND COAL SEAMS. *London, Engl. Univ. Press Ltd.*

SELLEY, R. C., 1970—Studies of sequence in sediments using a simple mathematical device. *Quart. J. geol. Soc. Lond.,* 125, 557-81.

STAINES, H. R. E., 1972—Blackwater Coalfield: Correlation of seams in the Rangal Coal Measures, Mackenzie River to Sirius Creek. *Geol. Surv. Qld Rep.* 70.

SWAINE, D. J., 1971—Boron in coals of the Bowen Basin as an environmental indicator. *Geol. Surv. Qld Rep.* 62, 41-8.

WHITE, M. E., 1969—Report on plant fossils from the Beaver Lake area, Prince Charles Mountains, Antarctica. *Bur. Miner. Resour. Aust. Rec.* 1969/100 (unpubl.).

WILLIAMS, P. R., 1971—Visit to Blackwater Mine, 7/3/71 to 14/3/71. *Rep. to Utah Devel. Co.* (unpubl.).

WILLIAMSON, I. A., 1967—COAL MINING GEOLOGY. *London, Oxford Univ. Press.*

APPENDIX 1

CHARACTERISTICS OF STRATIFICATION IN THE LOWER SANDSTONE, SOUTH WALL OF RAMP 5

Bed	*Maximum thickness (m)*	*Type of stratification*	*Grouped or solitary*	*Set size (cm)*	*Grainsize*	*Carbonaceous material*	*Shape of lower bounding surface*	*Nature of lower bounding surface*
A	1.65	X	G	15	m	r-a	T	E
B	1.65	X	G	12	m	r-a	T	E
C	0.50	X	G	15	m	r-a	T	E
D	0.36	X	G	9	m	r-a	T	E
E	0.30	X	G	12	m-c	r-a	P	E
F	0.55	X	G	40	m	r-a	I	E
G	1.25	X	G	25	m	r-a	I	E
H	0.45	Xrd	G	2	f-m	Awd	T	E
I	1.75	X	G	15	m	r	T	E
J	1.15	X	G	22	m	rwd	T	E
K	0.38	X	G	20	m	r	T	E
L	0.71	X	G	8	m	r-a	T	E
M	0.91	X	G	—	m	r-a	T	—
N					Interbedded sandstone (f-m, X, G) and shale			
O	0.91	X	G	13	m	A	P	—
P	0.84	X	G	15	f-m	com	T	E
Q	0.61	X	G	8	f-m	vA	P	E
R	0.61	L	—	—	f	com	—	—

Key to Symbols

X—Cross-stratified
Xrd—Ripple-drift laminated
L—Laminated
G—Group cross-stratified
f—Fine-grained
m—Medium-grained
c—Coarse-grained
a—Absent
r—Rare
com—Common
A—Abundant
vA—Very abundant
wd—Fossil wood
T—Trough
P—Planar
I—Irregular
E—Erosional

APPENDIX 2

PETROGRAPHIC DESCRIPTIONS OF THE PELLET CLAYSTONE AND UPPER TONSTEIN

by W. Koppe

(Geological Survey of Queensland)

Pellet Claystone

The pellet claystone (lower tonstein) is a thin bed of medium brown kaolinite which contains brownish grey siderite pellets. The kaolinite displays a clouded linear arrangement parallel to bedding and contains disseminated fine carbonaceous material and almond-shaped masses about 0.2 m long of granular microcrystalline kaolinite. The pelletal appearance of the tonstein is produced by groups of fine siderite grains which form masses up to 4 mm across. Spheres of siderite up to 0.2 mm in diameter also occur in the tonstein and consist of radially arranged sector-shaped crystals. Dark concentric banding is confined to the outer margin of the spheres. Some subangular quartz grains up to medium sand-size are scattered through the kaolinite. A few carbonaceous laminae lie parallel to the bedding.

The composition of the pellet claystone based on a petrographic estimate of one thin section is: 72 percent massive kaolinite; 1 percent microcrystalline kaolinite; 19 percent granular siderite; 4 percent siderite spheres; trace quartz; trace apatite; and 4 percent carbonaceous material.

The following diagenetic sequence may have affected the lower tonstein:

massive kaolinite
siderite spheres
granular siderite
microcrystalline kaolinite

Upper Tonstein

The upper tonstein is a thin calcareous sandy bed of pinkish tan kaolinite. The microcrystalline kaolinite is cut by a network of finely crystalline grey calcite. Individual walls in the calcite network are typically 0.2 mm thick, and the square cells they delineate are commonly 0.2 mm across. Carbonaceous laminae up to 3 cm long lie parallel to bedding. Small siderite grains rimmed by calcite are scattered throughout the kaolinite or are concentrated near carbonaceous fragments. Angular grains of quartz and unaltered plagioclase also occur in the kaolinite.

A petrographic estimate based on one thin section gives the following composition for the upper tonstein: 47 percent calcite; 47 percent microcrystalline kaolinite; 3 percent granular siderite; 1 percent quartz; trace plagioclase (An 38); trace apatite; 2 percent carbonaceous material.

The following diagenetic sequence may have affected the upper tonstein:

massive kaolinite
microcrystalline kaolinite
granular siderite
calcite network and
calcite rims on siderite grains

APPENDIX 3

ABBREVIATIONS USED IN LITHOLOGICAL LOGS

Brown	brn
Carbonaceous	carb
Claystone	Clst
Concretion	Conc
Conglomerate	Cgl
Cross-bed	Xbd
Cross-stratified	xstratd
Dark	dk
Fine	f
Fossil	Foss
Granule	Grnl
Grey	gy
Group	gp
Inclusion	Incl
Interbed (ed)	Intbd, intbdd
Intrusion	Intr
Laminae (ated)	Lam, lamd
Lens	Len
Light	lt
Lower	low
Massive	mass
Matrix	Mtx
Mudstone	Mdst
Pebble	Pbl
Pellet	Pel
Poor (ly)	P
Sandstone	Sst
Shale	Sh
Siltstone	Sltst
Solitary	sol
Thin	tn
Upper	up
Very	v
Wood	Wd